

COMPUTATIONAL MODELING OF THE MIGRATION OF RADIOACTIVITY IN A POROUS MEDIUM

by

SOUBHADRA SEN
(Enrolment No: PHYS02200704006)

Indira Gandhi Centre for Atomic Research, Kalpakkam

*A thesis submitted to the
Board of Studies in Physical Sciences
In partial fulfillment of requirements
For the degree of*

DOCTOR OF PHILOSOPHY

of

HOMI BHABHA NATIONAL INSTITUTE



MARCH, 2013

Homi Bhabha National Institute

Recommendations of the Viva Voce Board

As members of the Viva Voce Board, we certify that we have read the dissertation prepared by **Soubhadra Sen** entitled “**COMPUTATIONAL MODELING OF THE MIGRATION OF RADIOACTIVITY IN A POROUS MEDIUM**” and recommend that it may be accepted as fulfilling the dissertation requirement for the Degree of Doctor of Philosophy.

_____ **Date:**

Chairman – Dr. B. Venkatraman

_____ **Date:**

Convener/Guide – Dr. N. Mohankumar

_____ **Date:**

Member – Dr. K. Velusamy

_____ **Date:**

Member – Dr. R. S. Keshavamurthy

_____ **Date:**

Examiner

Final approval and acceptance of this dissertation is contingent upon the candidate’s submission of the final copies of the dissertation to HBNI.

Date:

Place:

CERTIFICATE

I hereby certify that I have read this dissertation prepared under my direction and recommend that it may be accepted as fulfilling the dissertation requirement.

Date: 28/03/2013

(N. Mohankumar)

Place: Kalpakkam

Thesis Supervisor

STATEMENT BY AUTHOR

This dissertation has been submitted in partial fulfillment of requirements for an advanced degree at Homi Bhabha National Institute (HBNI) and is deposited in the library to be made available to borrowers under rules of the HBNI.

Brief quotations from this dissertation are allowable without special permission, provided that accurate acknowledgement of source is made. Requests for permission for extended quotation from or reproduction of this manuscript in whole or in part may be granted by the Competent Authority of HBNI when in his or her judgment the proposed use of the material is in the interests of scholarship. In all other instances, however, permission must be obtained from the author.

Date: 28/03/2013

Place: Kalpakkam

(Soubhadra Sen)

Ph.D Candidate

DECLARATION

I, hereby declare that the investigation presented in the thesis has been carried out by me. The work is original and has not been submitted earlier as a whole or in part for a degree / diploma at this or any other Institution / University.

Date: 28/03/2013

Place: Kalpakkam

(Soubhadra Sen)

Ph.D Candidate

To my family.....

ACKNOWLEDGEMENTS

First of all, I thank Dr. Baldev Raj, Shri. S. C. Chetal and Dr. P. R. Vasudeva Rao, the former and the present Directors of IGCAR for allowing me to pursue research for the Ph.D. degree at IGCAR. I am grateful to Shri. S. A. V. Satyamurthy, Director, EIRSG and Dr. R. Indira, the former head of RSD for their support. I am grateful to Dr. B. Venkatraman, Head, RSD and Associate Director, RSEG for his encouraging words and advices.

I am grateful to the members of my doctoral committee [Dr. N. Mohankumar (guide), Dr. B. Venkataraman (Chairman), Dr. K. Velusamy (member), Dr. R.S. Keshavamurthy (member)] for their guidance and help. The thesis has taken this present form due to the outstanding guidance that I have received from my doctoral committee.

I thank V. Rajagopal and S. Bhaskar of RSD, Dr. D.K. Mahapatra of SRI and John of SED for their co-operation and help. I am grateful to my colleagues R. Ramar, Ajay Rawat and Ms. P. Priyada of RSD for their support and help.

Finally I thank all my colleagues for the assistance they have provided.

Date: 28/03/2013

(Soubhadra Sen)

Place: Kalpakkam

CONTENTS

	Page No.
Synopsis	i
List of figures	x
List of tables	xi
List of publications	xii

Chapter 1

Introduction to the problem statement and literature survey

1.1 Introduction	2
1.2 Nuclear waste and its classification	3
1.3 A Description of the rock structure	5
1.4 Survey of the existing literature	8
1.4.1 Literature survey for the deterministic models for a single species	8
1.4.2 Survey of the existing literature for multiple species	15
1.4.3 Literature survey for the probabilistic models	16
1.4.4 Experimental data related works	19
1.5 Summary of the present thesis	20
1.6 References	27

Chapter 2

The parallel fracture model and the finite difference solution

2.1 Introduction	32
2.2 A brief survey related to the parallel fracture model	32

2.3	A physical picture of the model	35
2.4	The mathematical model	37
2.4.1	The governing equation for the fracture medium	38
2.4.2	The governing equation for the porous matrix	40
2.5	The FTCS Approach	45
2.6	The method of undetermined coefficients	46
2.7	The CN approach	47
2.8	The DF Scheme	48
2.9	The higher order compact finite difference scheme	49
2.10	The 4th order CN approach	52
2.11	A stability analysis	53
2.12	Results and discussions	56
2.13	Conclusions	57
2.14	References	62

Chapter 3

Pseudospectral solution of the deterministic parallel fracture model

3.1	Introduction	65
3.2	A brief survey of literature	66
3.3	The equations for radioactivity migration in a porous medium	69
3.4	The pseudospectral method	70
3.4.1	The Chebyshev pseudospectral method	71
3.4.2	The Legendre pseudospectral method	71
3.5	Remarks on stability analysis	73
3.6	Results and discussion	73

3.7 Conclusions	76
3.8 References	83

Chapter 4

Probabilistic estimation of the radioactivity migration

4.1 Introduction	86
4.2 A brief survey of literature	88
4.3 A description of our present model	89
4.4 Results and discussions	93
4.5 Conclusions	94
4.6 References	99

Chapter 5

Numerical experimentation with the CN scheme

5.1 Introduction	101
5.2 The CN and the ICN scheme	101
5.3 The GCN scheme	102
5.4 Test problems	105
5.5 The migration of radioactivity in a porous medium	107
5.6 Conclusions	108
5.7 References	113

Chapter 6

Conclusion and outline of the future work

6.1 Chapter wise summary of the thesis	115
6.2 Outline of future work	118

SYNOPSIS

The need for clean and reliable sources of energy hardly needs an emphasis. The present sources of fossil fuels are rapidly getting depleted and at the same time, the burning of these fuels causes serious pollution problems. Hence we are forced to look at alternative routes of power generation (like nuclear, wind and solar). Harnessing the solar energy needs huge land area along with a reasonably high initial investment. The requirement of minimum wind velocity puts a restriction on the large scale wind power generation. Till the fusion based reactors become a reality, for India with its large thorium reserves, the nuclear route offers a viable source of energy.

During the operation of a fission reactor, U-235 and Pu-239 atoms undergo fission which generates energy and radioactive fission products. At the end of the operation, the spent fuel rods are taken out of the reactor and they are subjected to reprocessing. Elements like U and Pu are separated and one is left with low, intermediate and high level wastes. For example, the liquid wastes are classified as exempt (below 37 Bq/L), low level ($37-3.7 \times 10^6$ Bq/L), intermediate-level ($3.7 \times 10^6-3.7 \times 10^{11}$ Bq/L) and high-level waste (more than 3.7×10^{11} Bq/L) ^[1]. The low and intermediate level solid wastes are made into a slurry and kept in near surface trenches for about 100yrs in stringent isolation and after another 200 yrs of milder isolation, they are made harmless. Here we are concerned with the high level wastes that are relatively low in volume but their activity is very high.

The high level waste is first concentrated and then vitrified into a glass matrix. These glass matrices are sealed in canisters and then buried inside the earth surface at a depth of 500m or more. The medium surrounding these canisters is rock which is the porous medium that we discuss in subsequent chapters. In the event of a breach of the canister, the active waste will come in contact with the rock and propagate through its

pore water. A realistic model of this waste migration is needed practically as an environmental problem. This model has a local context. The spent fuel rods of FBTR are kept in a cooling tank of depth 20m. This tank has a steel lining. In the event of a combined clad and the steel lining failure, there will be a migration of the activity into the surrounding charnokite rock. This again calls for a modeling.

A rock is a combination of randomly oriented and interconnected fractures and porous blocks. The porous blocks are of arbitrary size and they are surrounded by the fracture network. If the radioactive waste comes into contact with the pore water, it will start migrating due to the combined effect of advection and mechanical dispersion through the fracture network within the rock. Moreover, the adsorption into and the desorption from the porous matrix-fracture interface also plays a role in the migration process. In addition, there will be a diffusion of the species from the fracture into the porous matrix. Neretnieks^[2] was the first to point out this important fact that the migration of the species could be greatly reduced due to the retardation effect of the matrix diffusion.

There are two routes to model this problem. One can assume a simplified structure (a neat geometry consisting of an infinite array of identical parallel fractures between which porous matrices of equal width are sandwiched) and set up a set of coupled partial differential equations (pde's) to describe the migration process. Tang et al.^[3] described the migration using a set coupled pde's for a linear fracture of infinite length. This was extended by Sudicky and Frind^[4] and their model is taken as the standard parallel fracture model. This model consists of an infinite array of periodically repeating identical parallel fractures separated by porous matrices. Chen and Li^[5] improved this model by introducing a proper inlet condition. Now the set of coupled pde's describing the migration can be solved by the Laplace transformation technique for a source of

constant strength. The solution is in the form of a two dimensional integral. The highly oscillatory nature of this solution integrand puts a restriction on the evaluation of this integral. One can obtain the concentration values for a maximum distance of about 200m in quadruple precision for a period of 1000 years. In reality, one needs the concentration values at distances of the order of 500m. Mohankumar et al.^[6,7] overcame these difficulties of the Laplace transform approach by resorting to finite difference solution of these pde's. They used both the FTCS and the Crank-Nicolson schemes. It is to be noted that the accuracy of this finite difference solutions is controlled crucially by the degree of approximation of an interface derivative term.^[8]

The second route is the probabilistic estimation of the migration within the random structure of a rock. Williams^[9] reports a method based on an analogy with the transport of neutron inside a non-multiplying medium. He assumes that the species undergoing a random walk inside the fracture network can change direction only at the intersection of two or more fractures. This point is termed as a node and the change of direction of the motion is considered as a pseudo-scattering event. The mechanism of diffusion from the fracture into the porous matrix is not considered here. Cvetkovic et al.^[10] reported a method to estimate the escape probability of the waste from a rock sample. Giacobbo and Patelli^[11] made a monte carlo based estimation of the radioactivity migration. They introduced the adsorption and desorption mechanisms in their model.

A comprehensive modeling of the radioactivity migration in rock using both the deterministic and the nondeterministic routes forms the main theme of this thesis work. The numerical schemes capable of providing reliable and highly accurate solutions are utilised to obtain solutions for the deterministic parallel fracture model. In addition, a random walk based approach is developed through a probabilistic route to model the problem in a more realistic way. The thesis consists of six chapters. Below a brief

description of the chapters is provided.

Outline of the thesis:

Chapter 1: In this chapter the context in which the present problem of the thesis arises and its importance to assess certain radiological and environmental related questions are highlighted. An outline of the problem and a survey of the literature related to the deterministic and the non-deterministic models of this porous flow problem are provided. This chapter also contains a chapter wise summary of the thesis.

Chapter 2: In this chapter, a detailed derivation of the parallel fracture model of Sudicky and Frind ^[4] is given along with its assumptions, initial, boundary and inlet conditions. The exact analytical solution and its limitation are then described. Subsequently, the finite difference solutions of Mohankumar et al. ^[6,7] using the FTCS and Crank-Nicolson (CN) schemes that are at best second order in space and time variables are described. One of the key aspects of the present thesis is to develop algorithms that will provide accurate solutions for larger distances and longer times. Specifically, three different finite difference schemes are implemented. They are the Dufort-Frankel (second order accurate both in space and time), the higher order CN and the Higher Order Compact Finite Difference schemes. The last two methods are fourth order accurate in space and second order accurate in time. A detailed comparison of all the schemes is given and the results establish the fact that the higher order CN and the Higher Order Compact Finite Difference scheme are best suited for the required estimation and they provide a reliable assessment of the concentration up to a distance of around 500m.

Chapter 3: The finite difference schemes that are dealt with in the previous chapter provide solutions that are at best accurate to fourth order in the space variable.

Also, the run times are large and the memory requirements are very heavy for reasonable accuracy. This raises an obvious question about the utilization of alternative schemes that provide better accuracy but with reduced memory requirement. This chapter provides an answer to these questions affirmatively. The prescription that is indicated is the use of the pseudospectral scheme. For our deterministic parallel fracture model, the Chebyshev and the Legendre pseudospectral methods are implemented and they are shown to yield far more accurate solutions than the finite difference schemes. Also, the run times and the memory requirements are reduced very drastically. These benefits stem essentially from the exponential convergence of these schemes that employ relatively fewer basis functions. But this method has a limitation. Let C_0 be a reference concentration to start with. In the pseudospectral method, a concentration value lesser than $C_0 10^{-16}$ can not be computed in double precision. The distance at which the concentration falls to this level gives the maximum distance of evaluation and this happens to be about 200m for our present set of parameters. By resorting to quadruple precision, this distance can be extended to about 300m. In conclusion it can be stated that for distances up to 300m, the pseudospectral method is the method to be employed. For distances beyond 300m, either the higher order CN or the higher order Compact finite difference schemes can be employed. Thus the pseudospectral methods and the above mentioned higher order finite difference schemes together provide a reliable algorithmic package for our concentration assessment.

Chapter 4: The deterministic model of the previous chapters assumes a simplified model of the rock. If one is interested in a more realistic estimation of the migration process, the flow through the random structure of a rock is to be modeled. A real rock is a combination of porous blocks and randomly oriented interconnected fractures. The intersection point of two or more fractures is called a node. Now if a

species is allowed to travel through such a network, at each node it will randomly choose any one of the available outlets. Thus the path it chooses between the source and the observation point is totally random and hence the total path length is a sum of the lengths of several zigzag paths and this sum is called the migration length. This length is always higher than the linear distance of separation between the source and the observation point. We make an estimation of the average migration length using the concept of random walk by averaging over several trials. Another important component of this model involves the diffusion of radioactive species through the porous blocks. This part is very difficult to model through the probabilistic route. For a small domain, this can be done using the Monte Carlo technique. But for the present problem it involves simulation over a large scale and hence it is impractical. We can circumvent this difficulty by adopting our earlier deterministic model for this part and hence we blend the best of both the deterministic and nondeterministic routes. Thus the calculations are performed using the deterministic parallel fracture model where we replace the linear fracture length by this average migration length. In these calculations, another important factor is the average width of the porous matrix. From the random distribution of the fractures, we estimate the maximum and the minimum possible widths of a porous matrix. We choose equispaced values in this range as equally probable representative values of width that are used in the deterministic calculation. We provide a comparison of the results of the probabilistic and the deterministic approaches. As expected, the probabilistic estimation proves to be more realistic and less conservative.

Chapter 5: In this chapter we report numerical experiments involving the CN scheme. The CN scheme is an unconditionally stable method and is capable of providing second order accuracy both in the space and the time variables for a purely diffusion problem. The second order accuracy in the space domain comes from the central

differencing approximation whereas the same order of accuracy in the time domain is due to the averaging of the spatial approximations between two levels of time. Let j be time index. Then in the conventional CN scheme, the centering is done between two time levels indicated by j and $(j+1)$. This can be referred to as the half-integer centered CN scheme. There is another variant of CN method where the averaging is done between $(j+1)$ and $(j-1)$ time levels. This can be termed as the integer-centered CN scheme. We discretise the diffusion equation by both the schemes and then average them arithmetically to arrive at a new discretised equation. We term this as the generalized CN scheme. The stability analysis shows that this is also an unconditionally stable method for the diffusion problem. Compared to the two conventional CN schemes, the amplification factor of the error (from the Fourier stability analysis) of the new scheme for the diffusion equation is smaller. Hence there exists a possibility of an onset of early convergence (i.e. the onset of solutions with a larger time step) for the new method. We have solved two test problems and the deterministic porous flow equations using this new scheme. In all the cases, this method has an early convergence trend when compared to the other two conventional CN schemes. However, the time step for normal accuracies is not reduced when compared to the other two methods. That is, it does not provide an eventual time step advantage. However, the solutions for complicated problems using this method prove to be definitely better as in the case our porous flow. This can be attributed to the better averaging while preserving the related symmetries in time and space discretisation. More extensive studies are required to explore the other advantages offered by this method.

Chapter 6: In this chapter the future direction of research are indicated. It has been remarked that the present analytical solution for the parallel fracture model needs a constant source assumption. It may be possible to derive a series based analytical solution

that does not involve this assumption. Also, for the constant source parallel fracture problem, the derivation of the present Laplace transform based solution is quite complicated. There exists a possibility of reducing the complexity of the derivation by the use of a group theoretical analysis. This may also provide more general solutions. Our random walk model, assumes a constant velocity and a fixed fracture radius. These assumptions may be relaxed in a future model if the computational complexities do not turn out prohibitive. The random walk methodology provides a less conservative estimate of the concentration than the deterministic model due to the increased path length from the source to the observation point. The question still remains as to how close these models are to real physical systems. These aspects can be resolved only by experiments. Finally, the generalized CN scheme needs to be explored further for exploiting its full potential.

References:

- [1] K. Raj , K.K. Prasad and N.K. Bansal, Nucl. Eng. Des. 236 (2006) 914.
- [2] I. Neretnieks, J. Geophys. Res. 85 (1980) 4379.
- [3] D.H. Tang, E.O. Frind and E.A. Sudicky, Water Resour. Res. 17 (1981) 555.
- [4] E.A. Sudicky and E.O. Frind, Water Resour. Res. 18 (1982) 1634.
- [5] C.T. Chen and S.H. Li, Waste Manage. 17 (1997) 53.
- [6] N. Mohankumar and S.M. Auerbach, Comput. Phys. Commun. 161 (2004) 109.
- [7] N. Mohankumar, Ann. Nucl. Energy 34 (2007) 222.
- [8] N. Mohankumar and S. M. Auerbach, Comput. Phys. Commun. 179 (2008) 773.

[9] M.M.R. Williams, Ann. Nucl. Energy 19 (1992) 791.

[10] V. Cvetkovic, S. Painter and J.O. Selroos, Nucl. Sci. Eng. 142 (2002) 292.

[11] F. Giacobbo and E. Patelli, Ann. Nucl. Energy 35 (2008) 1732.

List of figures

Figure No.	Caption	Page No.
Fig. 1.1.	Schematic picture of a rock.	5
Fig. 1.2.	Schematic picture of fracture, node and porous matrix.	7
Fig. 1.3.	Fracture and waste matrix geometry in a deterministic parallel fracture model.	11
Fig. 4.1	Estimation of the maximum width of a porous matrix	92
Fig. 4.2	Concentration vs. distance plot for $2B = 1$.	96
Fig. 4.3	Concentration vs. distance plot for $2B = 5$.	97
Fig. 4.4	Concentration vs. distance plot for $\varphi_{max} = 30^\circ$	97
Fig. 4.5	Concentration vs. distance plot for $\varphi_{max} = 60^\circ$	98
Fig. 4.6	Concentration vs. distance plot for $\varphi_{max} = 89^\circ$	98

List of tables

Table No.	Caption	Page No.
Table 1.1	Classification of the solid wastes.	26
Table 1.2	Classification of the liquid and the gaseous wastes	26
Table 2.1	Experimental values of the pore diffusivities (D_p)	58
Table 2.2:	Typical experimental values of pore diffusivity (D_p) and hydraulic conductivity (K_p) at different depths	59
Table 2.3	Typical pore size values	59
Table 2.4	The concentration values and the relative percentage errors at different distances by different methods	60
Table 3.1	Comparison of the concentration values calculated by the two pseudospectral methods	77
Table 3.2	Relative percentage errors of different methods	79
Table 3.3	Comparison of concentration values calculated by the Chebyshev pseudospectral method and the HOC scheme (for a period of <i>100yrs</i>)	80
Table 5.1	The concentration values at different distances by conventional CN, GCN and ICN methods (test problem 1)	110
Table 5.2	Concentration values at different distances by conventional CN, GCN and ICN methods (test problem 2)	111
Table 5.3	Concentration values at different distances by conventional CN and GCN (the porous flow problem)	112

List of publications

Published:

1. S. Sen and N. Mohankumar, “A computational strategy for radioactivity migration in a porous medium”, Ann. Nucl. Energy 38(2011) 2470.
2. S. Sen and N. Mohankumar, “A note on higher order numerical schemes for radioactivity migration”, Ann. Nucl. Energy 49 (2012) 227.

Communicated:

1. S. Sen and N. Mohankumar, “Migpore, A code package for the estimation of migration of radioactive species in a porous medium” (communicated to Comput. Phys. Commun.)
2. S. Sen and N. Mohankumar, A random walk based methodology for the realistic estimation of radioactivity migration in a porous medium (communicated to Ann. Nucl. Energy)

Chapter 1

Introduction to the problem statement and literature survey

1.1 Introduction

1.2 Nuclear waste and its classification

1.3 A Description of the rock structure

1.4 Survey of the existing literature

1.4.1 Literature survey for the deterministic models for a single species

1.4.2 Survey of the existing literature for multiple species

1.4.3 Literature survey for the probabilistic models

1.4.4 Experimental data related works

1.5 Summary of the present thesis

1.6 References

1.1 Introduction

The need for sources of energy with minimal environmental and pollution related consequences in the long run is a perennial theme occupying the human minds presently. This assumes even more significance due to the steady depletion of the known fossil fuel reserves. Till a fundamental breakthrough occurs in the successful harnessing of energy from the nuclear fusion based reactors, the wind, the solar and the nuclear routes offer proven possibilities alongside the conventional hydel, coal and oil based power generation. The energy generation from the wind and the sun is clean and free but it calls for a huge initial investment. The requirement of a minimum wind speed puts a restriction on the duration of availability from a wind based generation. Typically, in India such a minimum speed is guaranteed for about five months at best in a given year and that too at few selected locations mostly in the neighborhood of the western ghat regions. It must be noted that the solar energy generation on a large scale needs expensive solar panels and storage batteries and also needs a huge land area which may be prohibitive. In this context the fission based nuclear reactors offer a viable source of energy in times to come. They are in operation for more than fifty years.

The nuclear fission reactors are of two types, namely thermal and fast reactors depending upon whether the fission that takes place inside a reactor is due to a fast or a slow (thermalized) neutron. There are multiple layers of safety from design to operation that are provided in these reactors ^[1]. In addition to design, the safety of the personnel during a normal operation is guaranteed by an appropriate radiation shielding. The time one works in a radiation zone and the distance one maintains with respect to a radiation

source are well regulated so as to result in a safe and acceptable radiation exposure. Stated concisely, the radiation safety of the personnel working in a reactor is ensured by the following three factors, time, distance and shielding. In a similar fashion, the safety of the general public living in the vicinity of a reactor is taken care of by stringent design criteria and operational procedures. Still, the general public may have certain genuine apprehensions that can be easily clarified.

1.2 Nuclear waste and its classification

One of the public concerns about the operation of nuclear fission reactors is the aspect of long term safe disposal of the radioactive waste from the fission products. In the Indian context, this key aspect is taken care of with due diligence^[2]. Radioactive waste is broadly classified as low, intermediate and high level wastes. Tables (1.1, 1.2) give a classification for the above three levels for the solid, the liquid and the gaseous wastes. More details can be found in the paper of Raj et al.^[2]. The waste disposal method in India follows the three guidelines.

- The delay and the decay of short lived radionuclides.
- The concentration and the containment of radioactivity as practically as possible.
- The release of the low level radioactivity to the environment after a sufficient dilution and dispersion.

The gaseous waste treatment consists of an elaborate off-gas cleaning system consisting of wet scrubbers like the venturi, the dust, the packed bed, the cyclone separators, the high efficiency low pressure drop demisters, the chillers and the high

efficiency particulate air (HEPA) filters that retain practically most of the particulate radionuclides. The low level waste produced by the reactor operations, the off-gas scrubbers, the active floor drains, the decontamination centers and the laboratories is first treated to reduce its concentration. This involves a variety of processes like a chemical treatment for a co-precipitation, a selective ion-exchange for the radionuclide separation (using the synthetic zeolites, the granulated AMP etc.) and an evaporation for a very high volume reduction. In addition, one employs a membrane process like a reverse osmosis and an ultra filtration for a reduction of the liquid contamination. Once the liquid waste is treated to reduce the contamination to acceptable levels, then it is discharged.

The low and intermediate solid wastes are first subjected to a cementation and a polymerization for immobilization and after this they are stored in a shallow land repository that is subjected to an active control involving monitoring, surveillance and remedial work over a period of *100 yr*. This is followed by a *200 yr* of passive control that involves permanent markers and land use restrictions. These measures enable the decay of the activity to harmless levels.

High level and alpha contaminated liquid waste from the spent fuel processing and the radio metallurgical operations are first concentrated by an evaporation and then stored in stainless steel tanks. After sufficient cooling this waste is immobilized typically in a borosilicate matrix by a vitrification process. Subsequent to an interim retrievable storage with cooling, the container containing this glassy waste material is buried in deep geological formations at a depth of about *500m* to *600m*. At these depths, the medium

surrounding the waste containers is rock. In case of an accidental breach of a container, the waste matrix will become a radioactive source. *The aim of this thesis is to model as accurately and realistically as possible, the migration of the radioactivity in a porous rock medium in the relatively unlikely event of a breach of a container in its subterranean storage.* One can easily understand the environmental and the radiological consequences of this event that calls for a thorough investigation.

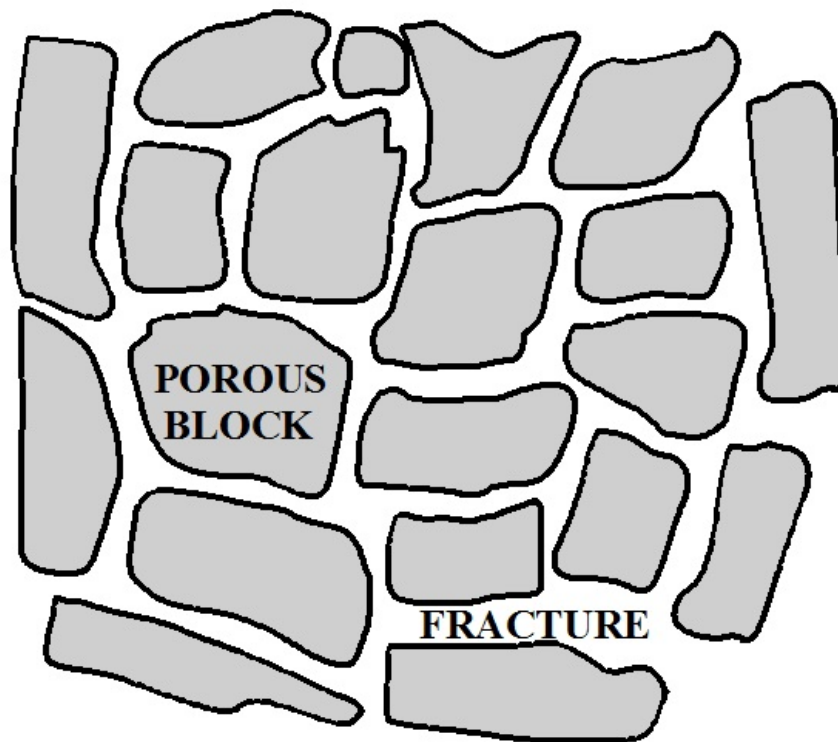


Fig. 1.1: Schematic picture of a rock.

1.3 A description of the rock structure

The rock consists of randomly distributed and interconnected pathways of tiny width called fractures through which the pore water migrates. These fractures are embedded in porous matrices of randomly varying sizes. If the waste matrix comes into

contact with the rock, the pore water will serve as a medium through which the radioactive species will migrate by a combination of advective and dispersive transport. The sorption of the species onto the surfaces of the fractures is also a mechanism that needs to be taken into consideration. In a seminal paper, Neretnieks^[3] was the first to point out the importance of the diffusion of radionuclides into the porous matrix. The importance stems from the fact that the migration of the species could be *retarded* to a very large degree if this mechanism of porous matrix diffusion is taken into consideration in addition to the sorption at the pore surface and the advective and the dispersive transport along the fractures. If diffusivities of appropriate magnitude for this process are supported by experimental evidence, then as pointed out by Neretnieks^[3], *few hundred meters of good rock will be a most effective barrier for most of the radionuclides of importance in a spent nuclear fuel.*

Figs. (1.1, 1.2) offer a typical picture of a rock with its random and interconnected fractures. As one can see, the length, the orientation and the width of the fractures are random variables. The radionuclide can be transported by the pore water in a solute form. From practical considerations, many models assume that the radionuclide gets instantly dissolved in the pore water and then migrates. More complex models have a provision for a non equilibrium that exists between the dissolved and the sorbed parts of the solute^[4]. The time dependent concentrations of the dissolved and the sorbed components are then determined by solving a rate equation. One has to treat the fracture length, the branching angle (the angle a fracture makes at a node) and the fracture width as random variables and then model the migration through a random walk process that will constitute a

nondeterministic model. In addition, the actual values of these important rock parameters must be experimentally determined to serve as absolutely necessary input data.

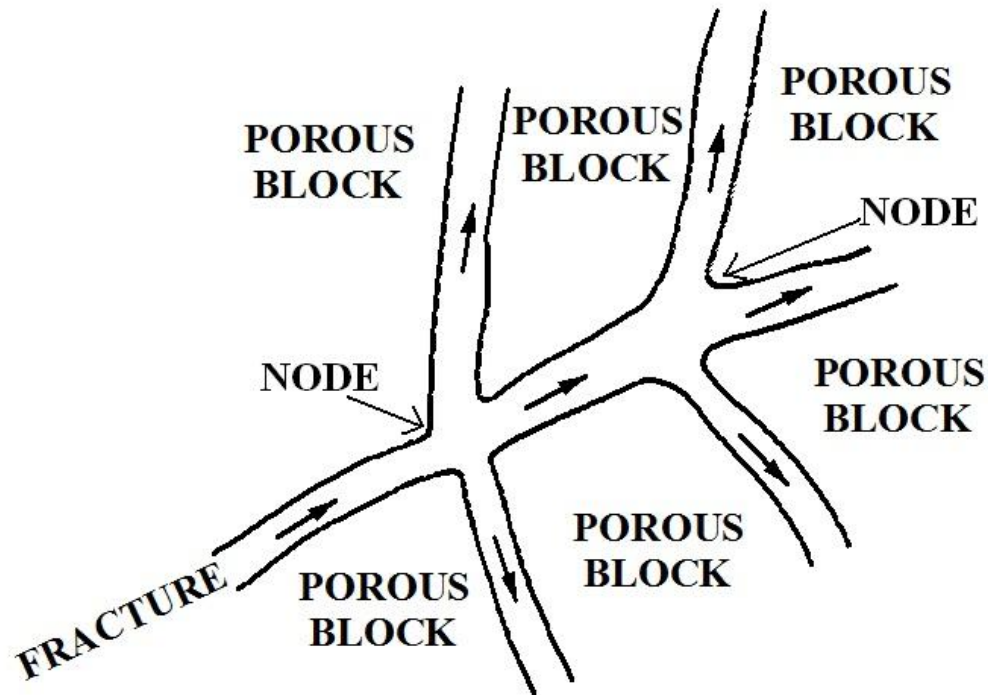


Fig. 1.2: Schematic picture of fracture, node and porous matrix.

Another widely followed approach to model the migration involves a deterministic route. Here the fractures are assumed to be straight lines and are of uniform width and they are parallel. This is illustrated in fig. (1.3). The source which is a radioactive matrix is located at one end and one is required to estimate the concentration along the fracture direction. Along a fracture, an advective, a diffusive and a radioactive decay component are involved. And in the transverse direction, a diffusion into the porous matrix and a radioactive decay are both included. *This deterministic model for a single radionuclide basically amounts to solving a pair of coupled partial differential*

equations, one for the concentration along the fracture and the other for the migration in the porous matrix. The present thesis explores and compares both the deterministic and the nondeterministic models.

The transport through a fracture involves both a mechanical dispersion and a molecular diffusion. The mathematical expression that describes this combination of two transport modes can be cast in the form of a diffusive transport. Hence for a transport along a fracture we use the terms either dispersive or diffusive but they both refer to a mechanism that involves both a mechanical dispersion and a molecular diffusion.

1.4 Survey of the existing literature

Here we present a comprehensive literature survey that encompasses the experimental observations, the evolution of the mathematical models (both deterministic and nondeterministic) and the analytical and the numerical solution techniques. The literature pertaining to the pseudospectral methods and a new Crank-Nicolson scheme are incorporated in the respective chapters.

1.4.1 Literature survey for the deterministic models for a single species

The seminal paper of Neretnieks^[3] first brought out the importance of a diffusion in the porous matrix and its role in the retardation of migration. It also contains a model for the transport of the radionuclide in both the fracture and the porous matrix. For the porous matrix, the diffusion and the radioactive decay are considered. But for the transport along *a single fracture*, dispersion is not included. Grisak and Pickens^[5]

consider a 2- D system consisting of a single fracture and a porous matrix of finite extent and they do a finite element analysis of the system. Their study highlights the conditions under which the fracture flow dominates over the matrix diffusion. Very low matrix porosities, a small fracture spacing, a large fracture width and a high fracture flow velocity are the factors that will make the matrix diffusion less dominant.

The inclusion of a dispersion along the fracture was carried out by Tang et al. ^[6] who considered a fracture of infinite length embedded in a porous matrix. This results in two partial differential equations, one for the transport along the fracture and the other for the transport in the porous matrix. The coupling between these two equations is provided by a diffusive flux at the fracture-porous matrix interface and this can be viewed as a source term for the differential equation that describes the transport along the fracture. Sudicky and Frind ^[7] extended the work of Tang et al. ^[6] by introducing a system of parallel fractures instead of a single fracture. This model was further improved by Chen and Li ^[8] who just modified the inlet condition at the source end appropriately. The model of Sudicky and Frind ^[7] with this modified inlet condition can be viewed as the standard parallel fracture model that we will refer to throughout the thesis.

Sudicky and Frind ^[7] as well as Chen and Li ^[8] use a Laplace transform technique to arrive at an analytical solution. This solution is a closed form, elegant but difficult to evaluate two dimensional integral expression. It must be noted that in both these models, the source strength is assumed to be a constant. Also, the dissolved and the adsorbed components are in equilibrium and they are related by a linear relation involving k_f , the

distribution coefficient. The assumption of a constant source strength implies that these two models can be applied only to sources of constant strength or whose half-life is very large, like the transuranic species. Hence these models are inapplicable for the cases of *short-lived* species.

Hodginson et al. ^[9] developed a *1-D* model where the following mechanisms, advection, dispersion, kinetic and/or equilibrium surface sorption, diffusion into the rock matrix with an equilibrium bulk sorption and a radioactive decay were included. This model has flexible input and output boundary conditions. The final solution for the concentration of the species in the fracture is found by numerically inverting the analytical solution of a Laplace transformed transport equations. In this investigation, it is found that matrix diffusion is the primary retardation mechanism for the element neptunium with an input data from the Finnsjo site of Sweden.

Ray and Nair ^[10] studied a non equilibrium migration in a rock matrix from a repository. Their cylindrical repository of finite dimension consists of a canister and a barrier. With respect to the rock, the repository is treated as a line source. The migration through a barrier is governed by a diffusion and a decay. The migration in the rock is estimated by solving a *3-D* pde that accounts for a dispersion, a decay, an advection, a sorption and a desorption. The above equations along with another equation for a non equilibrium sorption process are solved by a Laplace transform technique. Rasmuson ^[11] derived analytical solutions for the migration in fractures. In this model, the porous

matrix is treated as a system of spheres and the usual mechanisms that are considered in the fracture and in the porous matrix are retained.

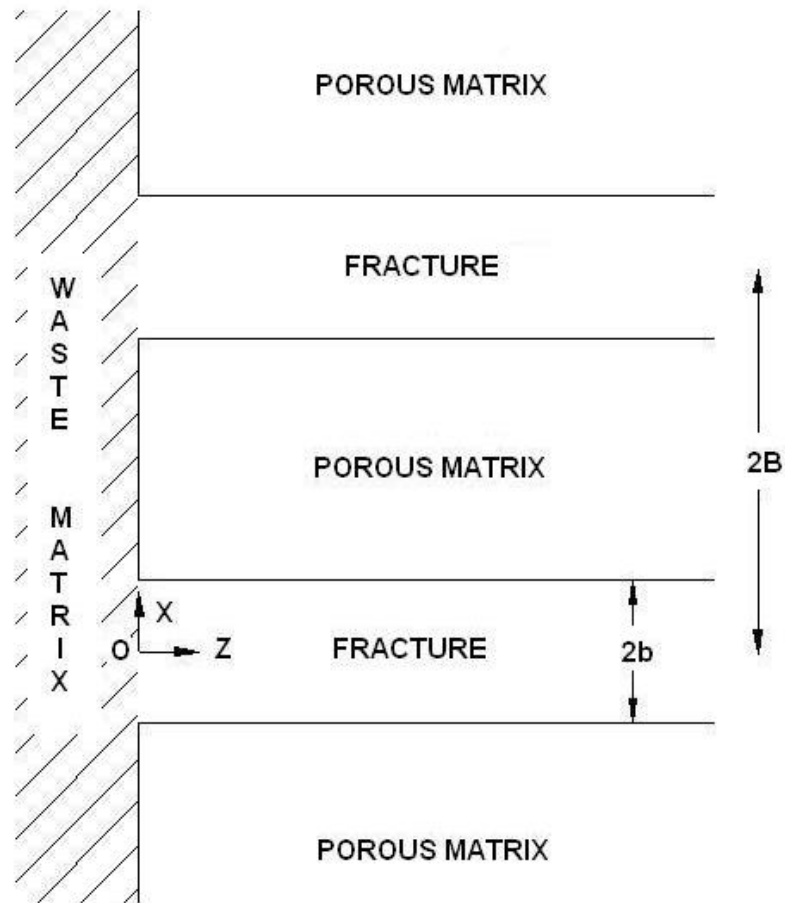


Fig. 1.3: Fracture and waste matrix geometry in a deterministic parallel fracture model.

Chen ^[12] models the radionuclide transport for a system consisting of an injection well, a single fracture and a porous matrix where the fracture and the porous matrix are of infinite extension. The source at an injection point is either a constant or an exponentially decaying one. The usual attenuation mechanisms like a radioactive decay and an adsorption with a linear equilibrium isotherm are incorporated. Along the fracture, an

advection and a dispersion are considered and the usual Laplace transform solution is presented. The simple migration model of Sharland et al. ^[13] consists of a waste, a backfill and the rock. Two differential equations, one for the radionuclide concentration in the water of the micro pores of the backfill and the other for the concentration in the rock water are solved by numerically inverting the Laplace transformed quantities.

Davis and Johnston ^[14] corrected some errors found in Sudicky and Frind ^[7]. Thomas ^[15] investigates a diffusional release of a single component material from a finite cylindrical waste that is kept in a well-stirred bath. The system has an azimuthal symmetry and hence r and z are the two independent variables. A Laplace transform solution is developed. The series for the Laplace transformed quantity is manipulated to handle an infinite summation efficiently before its inversion. Closed form expressions for the concentration profile, the flux through the ends, the fractional inventory leached and the leach rate are provided. Also, the governing equations have a provision for the inclusion of an irreversible reaction.

Chiou and Li ^[16] consider an exponentially decaying concentration as an inlet boundary condition and they provide an analytical solution for a single fracture and a porous matrix system. This is a more realistic inlet source condition since it can handle both long and short lived species without restriction. Their model also highlights the importance of the retardation factor that can influence both the fracture and porous matrix concentrations.

Chiou and Li's ^[17] work is essentially the same as that of Chiou and Li ^[16] except that the continuity of the flux across the fracture-source interface is altered to reflect a kinetic solubility limited dissolution condition (bc of the third kind).

Buckley and Loyalka ^[18] essentially consider a numerical solution to the above models of Chiou and Li ^[16, 17]. In addition, they consider a numerical solution for a 2-member chain for the same system. In this case, the analytical solution of Ahn ^[19] is compared. For the numerical solution, a centrally symmetric spatial finite difference scheme with a forward time discretization is employed. The analytical solution of Chiou and Li ^[17] is not valid if a variation of the velocity of the solute across the fracture occurs and such a situation exists when a reaction takes place at the fracture-porous matrix interface. The numerical scheme of Buckley and Loyalka ^[18] can however handle these scenarios with ease.

Buckley and Loyalka ^[20] place emphasis on the fact that the velocity across a fracture can be a variable instead of a constant as it is assumed in many models. Also, for a reacting flow, the assumption of a constant concentration across a fracture is not valid. They assume a parabolic velocity profile and consider a fracture in a two dimensional rock matrix defining a dual porosity model. The transport mechanisms considered in the fracture are an advection, a dispersion and a decay. A molecular diffusion, a decay and the adsorption/desorption are the physical processes that are considered for the surrounding porous matrix. These equations are solved by finite difference techniques

and the sensitivity of the results with respect to the mean velocity, the diffusion coefficients and the rate coefficients is discussed.

The continuum model of Jeong and Lee ^[21] is an interesting attempt to simplify the complexity of a porous medium. Here the random net work of fractures is replaced by two families of mutually orthogonal fractures. Each family consists of a set of periodically repeating parallel fractures of equal width inclined at 45 degrees to water flow. The mechanisms considered within the fracture and at the fracture rock interface are similar to those considered in standard models and the resulting equations are solved by a finite element technique. However, how closely this model mimics an actual fracture needs to be verified by actual experiments.

For a single fracture-porous matrix system, Lee and Teng ^[22] derive an analytical solution through a Laplace transform method. There are two pde's, one governing the migration through the fracture and the other one accounting for the transport through the porous matrix. The Laplace transform of the second equation gets modified depending upon the following three cases: (a) no sorption and a non equilibrium sorption; (b) an equilibrium sorption; (c) no sorption and an equilibrium sorption. Analytical solutions are presented for all the three cases.

Woodbury et al. ^[23] devise an interesting Arnoldi approach for the advection-dispersion equation to make it computationally more economical. In this formulation, instead of a system of n coupled differential equations, one has to deal only with a system

of m differential equations that describes the time evolution where $n \gg m$. Hence computational economy is enhanced without impairing the accuracy.

1.4.2 Survey of the existing literature for multiple species

The preceding section dealt with the migration models for a single species. Here we indicate few representative works that model the migration involving a chain of species. Burkholder and Rosinger ^[24] provide an explicit analytical solution for up to a three member chain through a geological media that involves an advection, a decay and with or without a dispersion. For a chain involving more than three members, this solution method will cut down the evaluation time since the chain can be grouped into a family of two or three member sets.

Huyakorn et al. ^[25] employ a finite element model to assess a nuclide decay chain transport in a naturally fractured porous medium by using a combination of a discrete fracture and a dual-porosity model. An advection, a hydrodynamic dispersion in the fractures, a diffusion in the porous matrix and the chain reactions of solute species are considered simultaneously in this formulation.

LeNeveu ^[26] devised a one dimensional migration model involving an advection and a dispersion for a chain of nuclides in a bentonite medium. A zero initial concentration of all the nuclides at time equal to zero is supplemented with a source boundary condition at $x = 0$ and another source-geosphere interface condition at $x = a$. After an exponential transformation, a Laplace transformation is applied and

subsequently a variety of analytical manipulations are implemented to efficiently calculate the series before inversion.

Hodgkinson and Maul ^[27] present a Laplace transform based solution to the radionuclide transport equations for decay chains of arbitrary length. Their fracture transport model includes a one dimensional advection, a linear equilibrium sorption, a hydrodynamic dispersion and the radioactive decay with a matrix diffusion for the fractured rock masses. This model has a provision for an approximate solution for the transport through a series of different types of rock.

Thomas ^[28] considers a case where a Green's function based solution is obtained for a chain of nuclides for a breach of a three dimensional repository. Here in the governing equation a convection, a dispersion and a retardation are considered. The contaminant inventory is preferentially released to a steady ground water flow. When all the radionuclides are equally mobile, a worst-case scenario is assumed and his method provides the bounding numbers. Also, one of the highlights of his approach is an ability to handle actinide chains of arbitrary length.

1.4.3 Literature survey for the probabilistic models

The probabilistic estimation of the migration of the contaminant particles through a porous medium is a widely established alternate route. Problems dealing with the dispersion and the diffusion have been dealt with using this approach since the middle of the last century ^[29, 30]. Ahlstrom et al. ^[31] developed a numerical code to simulate a

contaminant transport driven by a sub-surface flow. Kinzelbach ^[32] pointed out a dissimilarity between the conventional advection-diffusion equation and its random walk based variant for a heterogeneous system. The difference is small for a system with mild heterogeneity but the same becomes larger with an increase of the heterogeneity.

In modern times, the stochastic methods are widely used for different types of porous flow estimation. Sahimi and Jue ^[33] simulated a diffusion in a disordered porous medium. This corresponds to a Brownian motion of macro molecules. Their work established a correlation between the effective diffusion coefficient and the mean pore diameter of the medium. Frymier et al. ^[34] developed an algorithm to address the migration in a bulk system that is done as a series of zizzag segments. Berkowitz et al. ^[35] derived a general form for a conservative chemical transport in a geological matrix.

The resistance offered by a medium to a flow is known as permeability. For simple systems, Kozeny equation ^[36] gives a very simple and workable expression for the permeability. Simonov and Mascagni ^[37] made a detailed study of a complex digitized porous medium to establish a relation between the permeability and the diffusion penetration depth. A code (LAGCARTW) based on a random walk particle advection-diffusion model was developed by Sherwin ^[38]. This code can be run in a Windows environment. Nordbotten and Vasilyev ^[39] worked on the correlation between a multiple porosity model and a continuous time random walk. This work suggested that the continuous time random walk method could be viewed as a spatial discretization of a multiple porosity model in Lagrangian coordinates. Williams ^[40, 41] reported a stochastic

approach to model the migration of radioactive waste through a porous medium with fracture. This approach was based on an analogy with the neutron transport in a non multiplying medium. The numerical solution of this model was reported in a series of papers by Buckley et al. ^[42, 43, 44].

A simulation based on a Markov process (continuous in time) for a one dimensional transport of a radionuclide chain was carried out by Lee and Lee ^[45]. Smidts and Devooght ^[46] reported a method based on the concept of a non analog Monte Carlo simulation to model the transport of a chain in a geological medium. The issue of migration of a dissolved radionuclide has been addressed by Marseguerra et al. in a series of papers ^[47, 48, 49]. Marseguerra et al. ^[50] also estimated the effects of the engineered barriers of a radioactive waste repository using a Monte Carlo method. The Kolmogorov-Dmitriev theory ^[51] was used to simulate the flow of particles through different barriers. All the interactions that a particle could encounter during a transport process were considered as transitions from one particle state to another.

Cvetkovic and Haggerty ^[52] made a study of the transport of particles with an exchange in a disordered medium. The probabilistic model of Cvetkovic et al. ^[53] successfully incorporated the effect of the porous matrices in the evaluation of the concentration. Their results provided an estimation of the escape probability of a radionuclide from a rock. Bijeljic and Blunt ^[54] put forward an explanation for the complex macroscopic behavior of dispersion in a porous medium. They reported a relation between the longitudinal dispersion coefficient and the Peclet number.

Moreno et al. ^[55] pointed out that the uncertainty in the transport of the radioactive waste was mainly due to an uncertainty stemming from the retardation coefficients. In their assessment, they used the Palm process introduced by Mikhailov and Voitishk ^[56]. The Monte Carlo model of Giacobbo and Patelli ^[57] gave an estimation of the migration of radionuclide in a fractured porous medium. The effects of adsorption and desorption were considered with the incorporation of the porous blocks in the model. This description and that of Williams ^[40] gave identical results for a set of problems ^[57]. Zoia et al. ^[58] developed a method to describe the concentration-dependent transport of a contaminant particle in a porous medium using the concept of non linear random walk. This work was based on the dynamics of dense particles.

1.4.4 Experimental data related works

It needs hardly an emphasis on the central role of validated experimental data since it is central to every modeling. In this context, the work of Skagius and Neretnieks ^[59] provides the porosities and the diffusivities of some non sorbing species in crystalline rocks. The diffusion coefficient is modified to take into account the porosity, the tortuosity and the sorption effects. The surfaces in old fissures, that are in contact with the moving groundwater, are likely to have a different mineral composition than the surrounding rock. This is due to the weathering, the precipitates and the crystallization products from the groundwater. These modifications are termed as a coating material. The estimated diffusivities showed large differences between granite and gneiss taken from the same drilled core. This implies a practical impossibility of assigning a single value of the diffusivity for a rock material from a given area. Also their data indicates the

interesting point that the total diffusivity in rock with a fissure coating material is of the same order of magnitude or higher than the diffusivity in rock without a fissure coating material. Skagius et al. ^[60] did sorption experiments to evaluate the diffusion and the sorption parameters of cesium and strontium in granite samples from two different mines. Birgersson and Neretnieks ^[61] conducted experiments to find the rate of diffusion into the rock matrix. Migration was found to be different at different depths implying that the stress as a function of the depth could have a bearing on the migration. Also, the pore diffusivity and the hydraulic conductivity were found to have large variations with respect to depth.

1.5 Summary of the present thesis

Chapter 1: This first chapter has provided a comprehensive literature survey for the deterministic and the nondeterministic models.

Chapter 2: In the second chapter, the basic derivation of the governing equations of the parallel fracture model is indicated. This is followed by an application of the higher order finite difference schemes to these equations to get a reliable estimate of the concentration of the radionuclides for larger distances. The governing equations for the standard parallel fracture model were first set up by Sudicky and Frind ^[7] and subsequently, Chen and Li ^[8] used the same set of equations. But unlike Sudicky and Frind ^[7] who do not distinguish between the waste and the fracture sides, Chen and Li ^[8] label these two sides separately and provide an appropriate inlet boundary condition. Their analytical closed form solution is given as a 2-D integral by a Laplace transform

method. It has a very oscillatory integrand and hence its evaluation poses enormous difficulties. Also due to the finiteness of numerical precision, there is a limitation on the maximum distance from the source at which the concentration can be evaluated. In fortran double precision, these quadrature based calculations can be done for a distance of about $200m$. By resorting to quadruple precision, this distance can be extended a little more. This limitation served as a starting point to seek computational alternatives where the evaluation distance could be $500m$ or more. In this context, Mohankumar et al. ^[62,63] used the finite difference methods as a way of getting computational results for distance up to $500m$. They employed a Forward Time and Centered Space scheme (FTCS) ^[62] that gave a first order accuracy in time and a second order accuracy in the space variable. This was later improved by Mohankumar ^[63] who used a Crank-Nicolson (CN) scheme that gave second order accuracy in both the space and time variables.

This prompted the present thesis investigation to look for *higher order schemes* that will provide better precision than the FTCS and CN schemes at a reasonable computational cost. It is found that the higher order CN scheme can be profitably exploited to efficiently calculate the concentrations up to $500m$ with a *fourth order accuracy* in the space variable and a second order accuracy in the time variable. In recent times, the higher order compact schemes (HOCS) are extensively used in flow related problems ^[64, 65]. Taking clue from these works, the present porous flow equations are also solved by this HOCS approach. The order of accuracy of this HOCS approach is the same as that of the higher order CN method and hence they are comparable. These findings establish the fact that for distances up to $500m$, either of these two schemes namely the

higher order CN or the HOCS can provide reliable benchmark values through the deterministic route. Also, the CN, the higher order CN, the Dufort-Frankel (DF) and the higher order compact schemes were compared to assess their relative accuracies and performances. These findings were reported by Sen and Mohankumar ^[66, 67].

Chapter 3: In finite difference methods, one replaces a derivative by its approximant. Usually a derivative approximation amounts to a weighted linear combination of the function values in the neighborhood of the point of evaluation divided by the step size. In the pseudospectral method, we do not resort to a derivative approximation. Rather, the unknown is expressed as a linear combination of certain known functions belonging to a basis set. The expansion coefficients are then obtained by substituting this approximate solution in the given differential equation. Compared to the finite difference methods, the pseudospectral methods can offer a much superior accuracy, that is usually quantified as *an exponential convergence* ^[68]. This chapter explores the application of these pseudospectral methods for the radioactivity migration problem. The Chebyshev and the Legendre pseudospectral methods are employed for these computations. It is found that these methods offer far superior results compared to the finite difference methods. Due to a finite precision related restriction, the maximum distance of evaluation turns out to be about $300m$. Hence for distances not exceeding $300m$, the pseudospectral method is the method of choice while for distances exceeding $300m$, either the higher order CN or the compact schemes can be used. These findings were reported by Sen and Mohankumar ^[66, 67].

Chapter 4: In chapter four, we report a random walk based method for a more realistic and less conservative evaluation of the radioactivity migration. The parallel fracture model adopted for the deterministic calculation is a simplified picture of a real rock structure. In reality, rock is a combination of randomly oriented and interconnected network of fractures embedded within porous blocks of random size. A schematic of rock structure is given in fig. (1.1). In the deterministic model, one assumes a neat geometry where the fractures are assumed to be straight lines as shown in fig. (1.3). When a radionuclide travels through a fracture network of a real rock, it has to follow several randomly oriented zigzag paths. This increases the effective path length between a source and an observation point. Moreover the retardation within the porous matrix also increases with an increase in path length. The combined effect of these two mechanisms results in a very significant reduction of the concentration at an observation point when compared to the concentration calculated from a deterministic approach.

Williams ^[40, 41] reported a stochastic method to address the migration through a fracture network. This model did not have any allowance for a matrix diffusion. Later, Cvetkovic et al. ^[53] incorporated the diffusion mechanism that takes place within a matrix to estimate the escape probability of a radionuclide from a rock. The Monte Carlo model of Giacobbo and Patelli ^[57] considered the adsorption and the desorption processes to account for the retardation effect of a porous matrix.

Most of the existing models mainly consider an advective transport through a fracture network since this is the dominant mechanism. Though the model of Cvetkovic

et al. ^[53] considers matrix diffusion, the diffusion within a fracture is not considered. In a practical situation, it is very difficult to consider all the mechanisms within the framework of a probabilistic estimation due to the limitation of computer resources. So our main aim is to exploit the best of both the deterministic and the probabilistic routes to consider realistically all the transport mechanisms in a dual porous medium of fracture and porous matrix. To achieve this goal, we first estimate the path length using the concept of random walk. We make a number of trials to arrive at a mean path length between the source and the observation point. This quantity is called the average migration length. Once this is estimated, the fracture length of the deterministic parallel fracture model is set equal to this average migration length. Another important factor that determines the concentration at an observation point is the average width of a porous matrix. This quantity is fixed by estimating the maximum and the minimum possible block widths for a rock structure. With these two quantities as input, one can evaluate the concentrations using the standard parallel fracture model. The results of this model turn out to be less conservative as expected. Still, one needs an experimental verification to validate all these models.

Chapter 5: This chapter deals with some numerical experiments involving the CN scheme. One of the problems associated with the CN schemes is an inherent oscillation of the solution ^[69]. In this context, numerical experiments were carried out to explore the possibility of suppressing the oscillations by resorting to a *better averaging* without violating the time centering of the space and time derivatives. For the CN scheme, it must be recalled that a central differencing scheme is used for the space

derivatives and more importantly, the time and space derivative approximations center around a particular time node. The time derivative can be centered around an integer time node or around a half-integer time node. As an experimentation, we averaged the two CN schemes based on these two time centerings that resulted in a CN variant. This CN variant *did not* provide a time step advantage in the sense that it did not yield an increased time step compared to the conventional CN scheme for the same accuracy. But in few cases it demonstrated the onset of solution at very early times for some test problems involving a diffusion. Also, for our porous flow problem, the convergence of the new CN scheme is found to be definitely better. Here again, the ultimate converged values of the conventional CN and its variant do not differ. This method needs further analysis and experimentation to exploit its full potential.

Chapter 6: In the final chapter we summarize the results of the thesis and also point out some possible directions for the future research.

Table 1.1 : Classification of the solid wastes

Category	Radiation Dose (D) on the surface of the waste package (mGy/h)	Comments
I	$D < 2$	Beta-gamma emitters
II	$2 < D < 20$	Beta-gamma emitters
III	$20 < D$	Beta-gamma emitters
IV	Alpha bearing wastes	Activity in Ci/m^3 or Bq/m^3

Table 1.2: Classification of the liquid and the gaseous wastes

Type	Category	Activity (A) (Bq/m^3) (beta-gamma emitters)
Liquid	I	$A < 3.7 \times 10^4$
	II	$3.7 \times 10^4 < A < 3.7 \times 10^7$
	III	$3.7 \times 10^7 < A < 3.7 \times 10^9$
	IV	$3.7 \times 10^9 < A < 3.7 \times 10^{14}$
	V	$3.7 \times 10^{14} < A$
Gas	I	$A < 3.7$
	II	$3.7 < A < 3.7 \times 10^4$
	III	$3.7 \times 10^4 < A$

1.6 References

- [1] C.V. Sundaram and S.M. Lee, *Pramana* 24 (1985) 193.
- [2] K. Raj , K.K. Prasad and N.K. Bansal, *Nucl. Eng. Des.* 236 (2006) 914.
- [3] I. Neretnieks, *J. Geophys. Res.* 85 (1980) 4379.
- [4] R.L. Buckley, S.K. Loyalka and M.M.R. Williams, *Ann. Nucl. Energy* 22 (1995) 453.
- [5] G.E. Grisak and J.F. Pickens, *Water Resour. Res.* 16 (1980) 719.
- [6] D.H. Tang, E.O. Frind and E.A. Sudicky, *Water Resour. Res.* 17 (1981) 555.
- [7] E.A. Sudicky and E.O. Frind, *Water Resour. Res.* 18 (1982) 1634.
- [8] C.T. Chen and S.H. Li, *Waste Manage.* 17 (1997) 53.
- [9] D.P. Hodgkinson, D.A. Lever and T.H. England, *Ann. Nucl. Energy* 11 (1984) 111.
- [10] A.K. Ray and S. Nair, *Ann. Nucl. Energy* 11 (1984) 611.
- [11] A. Rasmuson, *Water Resour. Res.* 20 (1984) 1435.
- [12] C.S. Chen, *Water Resour. Res.* 22 (1986) 508.
- [13] S.M. Sharland and P.W. Taster, *Ann. Nucl. Energy* 13 (1986) 141.
- [14] C.B. Davis and C.D. Johnston, *Water Resour. Res.* 20 (1984) 1321.
- [15] G.F. Thomas, *Ann. Nucl. Energy* 14 (1987) 283.
- [16] S.L. Chiou and S.H. Li, *Nucl. Technol.* 101 (1993) 92.
- [17] S.L. Chiou and S.H. Li, *Nucl. Technol.* 104 (1993) 258.
- [18] R.L. Buckley and S.K. Loyalka, *Ann. Nucl. Energy* 20 (1993) 701.
- [19] J. Ahn, *Mass transfer and transport of radionuclides in fractured porous rock*, PhD Thesis, Uni-versity of California-Berkley, 1988.

- [20] R.L. Buckley and S.K. Loyalka, *Ann. Nucl. Energy* 21 (1994) 461.
- [21] J.T. Jeong and K.J. Lee, *Ann. Nucl. Energy* 19 (1992) 459.
- [22] C. H. Lee and S. P. Teng, *Nucl. Technol.* 101 (1993) 67.
- [23] A.D. Woodbury, W.S. Dunbar and B.N. Omid, *Water Resour. Res.* 26 (1990) 2579.
- [24] H.C. Burkholder and E.L.J. Rosinger, *Nucl. Technol.* 49 (1980) 150.
- [25] P.S. Huyakorn, B. H. Lester, and J.W. Mercer, *Water Resour. Res.* 19 (1983) 841.
- [26] D.M. LeNeveu, *Ann. Nucl. Energy* 14 (1987) 77.
- [27] D.P. Hodgkinson and P.R. Maul, *Ann. Nucl. Energy* 15 (1988) 175.
- [28] G.F. Thomas, *Ann. Nucl. Energy* 20 (1993) 809.
- [29] A.E. Scheidegger, *J. Geophys. Res.* 66 (1954) 3273.
- [30] G.D.J. de Jong, *Trans. Am. Geophys. Union* 39 (1958) 67.
- [31] S.W. Ahlstrom, H.P. Foote, R.C. Arnett, C.R. Cole and R.J. Serne, Rep. BNWL-2127, Battelle Pacific Northwest Lab., Richland, Washington, 1977.
- [32] W. Kinzelbach, *NATO ASI Series C*, 224 (1987) 227.
- [33] M. Sahimi and V. L. Jue, *Phys. Rev. Lett.* 62 (1989) 629.
- [34] P.D. Frymier, R.M. Ford and P.T. Cummings, *Chem. Eng. Sci.* 48 (1993) 687.
- [35] B. Berkowitz, J. Klafter, R. Metzler and H. Scher, *Water Resour. Res.* 38 (2002) 1191.
- [36] J. Kozeny, *Sitz.-Ber. Wiener Akad., Abt. IIa*, 136 (1927) 271.
- [37] N. A. Simonov and M. Mascagni, *Monte Carlo Methods Appl.* 10 (2004)

599.

- [38] T.J. Sherwin, *Mar. Model.* 1 (1999) 83.
- [39] J.M. Nordbotten and L. Vasilyev, XVIII International Conference on Water Resources, CMWR 2010, 1.
- [40] M.M.R. Williams, *Ann. Nucl. Energy* 19 (1992) 791.
- [41] M.M.R. Williams, *Ann. Nucl. Energy* 20 (1993) 185.
- [42] R.L. Buckley, S.K. Loyalka and M.M.R. Williams, *Ann. Nucl. Energy* 20 (1993) 203.
- [43] R.L. Buckley, S.K. Loyalka and M.M.R. Williams, *Ann. Nucl. Energy* 20 (1993) 421.
- [44] R.L. Buckley, S.K. Loyalka and M.M.R. Williams, *Ann. Nucl. Energy* 20 (1993) 569.
- [45] Y. Lee and K.J. Lee, *Ann. Nucl. Energy* 22 (1995) 71.
- [46] O.F. Smidts and J. Devooght, *Math. Comput.Simul.* 47 (1998) 461.
- [47] M. Marseguerra and E. Zio, *Ann. Nucl. Energy* 25 (1998) 1301.
- [48] M. Marseguerra, E. Patelli and E. Zio, *Ann. Nucl. Energy* 28 (2001) 777.
- [49] M. Marseguerra, E. Patelli and E. Zio, *Ann. Nucl. Energy* 28 (2001) 1779.
- [50] M. Marseguerra, E. Zio, E. Patelli, F. Giacobbo, P. Risoluti, G. Ventura and G. Mingrone, *Ann. Nucl. Energy* 30 (2003) 473.
- [51] A.N. Kolmogorov and N.A. Dmitriev, *C. R. Acad. Sci. URSS* 56 (1947) 1.
- [52] V. Cvetkovic and R. Haggerty, *Phys. Rev. E* 65 (2002) 051308.
- [53] V. Cvetkovic, S. Painter and J.O. Selroos, *Nucl. Sci. Eng.* 142 (2002) 292.
- [54] B. Bijeljic and M.J. Blunt, *Water Resour. Res.* 42 (2006) W01202.

- [55] J.M.D. Moreno, S. Lazaar and F.O. Gallego, C. R. Acad. Sci. Paris, Ser. I 345 (2007) 415.
- [56] G.A. Mikhailov and A.V. Voitishchek, Convergence of computational models of random fields connected with Palm point flows, Russian Acad. Sci. Dokl. Math. 1994.
- [57] F. Giacobbo and E. Patelli, Ann. Nucl. Energy 35 (2008) 1732.
- [58] A. Zoia, C. Lattille and A. Cartalade, Phys. Rev. E 79 (2009) 041125.
- [59] K. Skagius and I. Neretnieks, Water Resour. Res. 22 (1986) 389.
- [60] K. Skagius, G. Svedberg and I. Neretnieks, Nucl. Technol. 59 (1982) 302.
- [61] L. Birgersson and I. Neretnieks, Water Resour. Res. 26 (1990) 2833.
- [62] N. Mohankumar and S.M. Auerbach, Comput. Phys. Commun. 161 (2004) 109.
- [63] N. Mohankumar, Ann. Nucl. Energy 34 (2007) 222.
- [64] S. K. Lele, J. Comput. Phys. 103 (1992) 16.
- [65] A. Mohebbi and M. Dehghan, Appl. Math. Modell. 34 (2010) 3071.
- [66] S. Sen and N. Mohankumar, Ann. Nucl. Energy 38 (2011) 2470.
- [67] S. Sen and N. Mohankumar, Ann. Nucl. Energy 49 (2012) 227.
- [68] J.P. Boyd, Chebyshev and Fourier spectral methods, Lecture notes in engineering, Springer-verlag, Berlin, 1989.
- [69] D. J. Duffy, Wilmott Magazine 12 (2004) 68.

Chapter 2

The parallel fracture model and the finite difference solution

- 2.1 Introduction
- 2.2 A brief survey related to the parallel fracture model
- 2.3 A physical picture of the model
- 2.4 The mathematical model
 - 2.4.1 The governing equation for the fracture medium
 - 2.4.2 The governing equation for the porous matrix
- 2.5 The FTCS Approach
- 2.6 The method of undetermined coefficients
- 2.7 The CN approach
- 2.8 The DF Scheme
- 2.9 The higher order compact finite difference scheme
- 2.10 The 4th order CN approach
- 2.11 A stability analysis
- 2.12 Results and discussions
- 2.13 Conclusions
- 2.14 References

2.1 Introduction

This chapter provides a comprehensive treatment of the finite difference methods for the solution of the coupled partial difference equations (pde's) that govern the migration of the radionuclides in the fracture and in the porous matrix of rock within the framework of the parallel fracture model. The material is organized as follows. First the basic works that are of importance in the analytical and the numerical solution of this parallel fracture model are briefly described. This is followed by a detailed derivation of the coupled pde's that govern the migration of the radionuclides. The solution of these pde's by a higher order CN and the higher order compact finite difference (fd) scheme are then presented. These results form one of the main components of this thesis.

2.2 A brief survey related to the parallel fracture model

The isolation of the vitrified high level waste (HLW) for longer times is accomplished by storing them in containers in crystalline rock at depths of $500m$ or more. The rock has a very low permeability that is essentially governed by the fractures. Neretnieks ^[1] was the first to point out that diffusion in the rock matrix could very significantly retard the migration of the radionuclides. His model consisted of a single fracture and a porous matrix. He considered a diffusion and a radioactive decay as mechanisms in the porous matrix while in the fracture, only an advective and a radioactive decay component were considered. A similar model was considered by Grisak and Pickens ^[2]. It consisted of a 2-D system of a single fracture and porous matrix of finite extent. A finite element analysis was done that pointed out conditions under which the fracture flow would dominate over the matrix diffusion. Typically, very low

matrix porosities, small fracture spacings, a large fracture width and a high fracture flow velocity are the crucial parameters that will make the matrix diffusion less dominant.

Tang et al. ^[3] and Rasmuson and Neretnieks ^[4] were the first to include the effects of a longitudinal hydrodynamic dispersion in their modeling. It must be understood that the radioactive species in the fracture can exist in two forms, the dissolved component in the pore water and the adsorbed components in a solid form. By assuming an equilibrium, these two components are related by a linear relation involving k_f , the distribution coefficient. Under these assumptions, the governing pde's for the single fracture-porous matrix model of Tang et al. ^[3] are given below.

$$\frac{\partial C}{\partial t} + \frac{v}{R} \frac{\partial C}{\partial z} - \frac{D}{R} \frac{\partial^2 C}{\partial z^2} + \lambda C - \frac{\theta D_p}{Rb} \left[\frac{\partial C_p}{\partial x} \right]_{x=b} = 0 \quad (2.1)$$

$$\frac{\partial C_p}{\partial t} - \frac{D_p}{R_p} \frac{\partial^2 C_p}{\partial x^2} + \lambda C_p = 0 \quad (2.2)$$

where b is the semi width of a fracture. With C and C_p referring to concentrations in the fracture and in the porous matrix respectively, the first and second equations relate to the migrations along the fracture and the porous matrix, respectively. The second, the third and the fourth terms of the first equation account for the advection, the mechanical dispersion and the radioactive decay, respectively. The last term of the first equation accounts for the diffusive flux from the fracture into the porous matrix and this term provides a coupling between the two equations. The term v stands for the velocity of water in the fracture. D and R are the dispersion and the retardation coefficients respectively for the fracture while D_p and R_p are the corresponding parameters for the porous matrix. λ is the radioactive decay constant. Also, it must be noted that for the

migration in the porous matrix, only a diffusion and a radioactive decay are considered. The above equations must be supplemented with appropriate initial, boundary and inlet boundary conditions ^[3].

The models of Rasmuson and Neretnieks ^[4] and Rasmuson ^[5] are similar and these two models differ by their inlet boundary conditions. The physical mechanisms considered in these models are similar to that of Tang et al. ^[3]. Common to both these models is the assumption that a rock is made up of porous blocks that are separated by fissures. In three dimensions, this results in a cubic system of orthogonal fractures of equal width and spacing. For modeling purposes, the cubic block that constitutes the porous matrix is replaced by a sphere having the same surface to volume ratio. It must be noted that the block radius is small when compared with the overall distances we consider.

Sudicky and Frind ^[6] extended the single fracture model of Tang et al. ^[3] to a system of identical parallel fractures. In two dimensions, this results in fractures that are separated by the porous matrices. This system of fracture-porous matrix repeats periodically in space as shown in fig. (1.3). The waste matrix and the fracture-porous matrix system are separated by an interface located at $z = 0$. Here z is measured along the fracture and the z and x axes are mutually perpendicular. The inlet condition that is used in this model is given by $C(z,t)_{z=0} = C_0$ where C_0 is a constant. This implies a source of constant strength at the $z = 0$ end. These equations were solved by a Laplace transform method to yield an analytical solution in the form of a two dimensional integral. This

integral was evaluated by a quadrature since it could not be evaluated in closed form. However, it must be remarked that the evaluation of these types of integrals needs a great deal of effort owing to its extremely oscillatory integrand. Also, it must be kept in mind that as the distance of evaluation gets larger, the difficulty of evaluation increases in proportion. This model of Sudicky and Frind ^[6] with a modified inlet condition introduced by Chen and Li ^[7] is taken as the standard parallel fracture model that we use in our subsequent calculations. This improved inlet condition is as follows.

$$-D \left[\frac{\partial C}{\partial z} \right]_{z=0} + vC(0, t) = vC_0$$

Thus, the flux at the source side is equal to the sum of a normal advective flux plus a dispersive flux evaluated at the fracture side at the source-fracture interface. With this inlet condition, Chen and Li ^[7] provide an analytical solution to the pde's by a Laplace transform techniques. Again, one ends up with a two dimensional integral solution that is evaluable in principle but harder to evaluate in practice due to its highly oscillatory integrand.

2.3 A physical picture of the model

As we described in the previous chapter, the rock consists of a network of fractures that are randomly oriented. The length, the width, the angle a given fracture makes with a reference direction and the velocity of the water in the fracture etc. are truly random parameters that are site specific. There are two ways to treat this problem. One way is to develop a nondeterministic approach where all the random aspects of the structure will be taken care of by a random walk approach. This mode of attack will be taken up in a subsequent chapter. Here we consider a deterministic model where we

simplify the fracture-porous matrix geometry so that we end up with a set of coupled pde's that can be solved with appropriate inlet, initial and boundary conditions. This simplified deterministic model is the standard model of the parallel fracture that was described in the previous section and it is illustrated in fig. (1.3). Due to the inherent symmetry of this model, one needs to concentrate on a single fracture alone. The point $z = 0$ separates the fracture and the waste matrix. To be more precise, the waste matrix and the fracture sides are represented by $z = 0^-$ and $z = 0^+$, respectively. The assumptions of this model are listed below.

- All the fractures are identical with a width $2b$. Similarly, all the porous blocks are also identical. The midpoints of two consecutive fractures are separated by a distance $2B$.
- The length of a fracture is much larger than its width.
- The transverse diffusion and dispersion ensures a mixing within each fracture. We assume that no concentration gradient exists across the width of a fracture.
- The hydraulic conductivity of the porous rock matrix is very low and so it is assumed that the water flow takes place only within the fracture.
- The flow of water within a fracture is laminar.
- The flow velocity of water is same in all the fractures.
- The migration of the radioactivity within a porous block is governed by a diffusion only and it takes place in the direction perpendicular to the fracture axis.
- The migration along the fracture is faster than the migration within a porous matrix.

The first assumption relates to the geometry of the model. The second and the third ones indicate that a flow along a fracture is essentially a migration in one dimension. The fourth, the seventh and the eighth assumptions indicate that the transport within a porous matrix is governed by a diffusion only. Moreover, these assumptions allow a one dimensional analysis of the migration within the porous blocks. The fifth assumption enables the application of Darcy's law for the fracture transport. The sixth one is required for obtaining an analytical solution.

It is important to note that all the models require physical parameters that need to be found experimentally. These parameters are site dependent. Even within a given site, they vary from location to location. Tables (2.1 – 2.3) give a flavor of some of the important parameters that are obtained experimentally from the samples of Stripa mine, Sweden ^[8].

2.4 The mathematical model

We first discuss different transport mechanisms of a particle inside a porous medium.

- **Advective transport:** An advective (convective) transport of the dissolved species involves the migration due to the flow of water. If the transport is purely due to this mechanism (diffusion being absent), the dissolved particles move at the speed of water flow.
- **Diffusive transport:** Diffusion is a spontaneous process which tries to reduce the concentration gradient present in a medium and it is a dominant mechanism at low velocities.

- **Dispersive transport:** This occurs along the fracture axis. The mechanical dispersion describes the combined effects of mixing due to a velocity profile and a roughness of the fracture walls. It is due to the flow and the pore system present in a medium and it is a predominant transport mechanism at high velocities. Experiments show that the mathematical expression of dispersion is very similar to that of a diffusion process. Usually the dispersive process is defined by a parameter D that *combines the effects of dispersion and molecular diffusion* and it is given by

$$D = \alpha_L v + D^* \quad (2.3)$$

Here α_L is the dispersivity in the direction of the fracture axis and D^* is the molecular diffusion coefficient in water.

2.4.1 The governing equation for the fracture medium

Let us consider an elementary rectangle that has sides of magnitude $2b$ and Δz and this rectangle lies within the fracture between the points z and $(z + \Delta z)$. We consider a parallelepiped of unit height with this rectangle as the base and so it has a volume of magnitude $(2b\Delta z)$. We consider the flow of water that enters this volume through the face located at z and leaves at the other face located at $(z + \Delta z)$. With C as the concentration per unit volume in the water and S as the *solid concentration per unit length* of the fracture surface, then the quantities of the species within this elementary volume in the liquid and the solid form are given by $(2b\Delta zC)$ and $(2\Delta zS)$, respectively. Within this volume, it must be remembered that the solid component resides on both the sides of the

fracture wall and thus gets deposited on the two sides of total length $2\Delta z$. The rate of change of this quantity is given by

$$\frac{\partial}{\partial t} [(2b\Delta z C) + (2\Delta z S)]$$

Let v be the velocity of water through the fracture and it is assumed to be a constant. Then the net advective component of mass that enters this volume per unit time is given by

$$[2b(Cv)_z - 2b(Cv)_{z+\Delta z}]$$

Similarly the net dispersion related component of mass that enters the volume per unit time is given by

$$\left[-2bD \frac{\partial}{\partial z} (C) \Big|_z + 2bD \frac{\partial}{\partial z} (C) \Big|_{z+\Delta z} \right]$$

Let λ be the decay constant of the radioactive species. The loss due to the radioactive decay per unit time is given by

$$\lambda [(2b\Delta z C) + (2\Delta z S)]$$

Finally, we must take into consideration the loss due the diffusive flux from the fracture. This loss term is given by $(2\Delta z q)$ where q is the diffusive mass flux from the fracture into the porous matrix. The expression of q is given by

$$q(z, t) = -\theta D_p \left\{ \frac{\partial C_p}{\partial x} \right\}_{x=b}, \quad z \geq 0, \quad t \geq 0 \quad (2.4)$$

Here D_p and C_p are the coefficient of diffusion and the concentration of dissolved radioactive species within the porous matrix, respectively. θ represents the matrix porosity which indicates the fraction of the porous volume with respect to the total volume of the porous matrix. Collecting all the terms we get

$$\begin{aligned} \frac{\partial}{\partial t} [(2b\Delta z C) + (2\Delta z S)] = & \left[2b(Cv)_z - 2b(Cv)_{z+\Delta z} \right] + \left[-2bD \frac{\partial}{\partial z} (C)|_z + 2bD \frac{\partial}{\partial z} (C)|_{z+\Delta z} \right] \\ & - \lambda [(2b\Delta z C) + (2\Delta z S)] - 2\Delta z q \end{aligned} \quad (2.5)$$

Upon simplification we arrive at the following equation.

$$\frac{\partial}{\partial t} \left(C + \frac{S}{b} \right) = D \frac{\partial^2 C}{\partial z^2} - v \frac{\partial C}{\partial z} - \lambda \left(C + \frac{S}{b} \right) - \frac{q}{b} \quad (2.6)$$

We assume a linear relation between the dissolved and the solid components, C and S . Then they are related by an empirical constant k_f , known as the distribution coefficient in the following way.

$$S = k_f C \quad (2.7)$$

Let R denote the retardation coefficient of the fracture and this is defined as

$$R = 1 + \frac{k_f}{b} \quad (2.8)$$

Substituting eq. (2.7) and eq. (2.8) into eq. (2.6), one gets the following pde.

$$\frac{\partial C}{\partial t} + \frac{v}{R} \frac{\partial C}{\partial z} - \frac{D}{R} \frac{\partial^2 C}{\partial z^2} + \lambda C + \frac{q}{Rb} = 0, \quad z \geq 0, \quad t \geq 0 \quad (2.9)$$

This is the first reference equation for the transport through the fractures for our standard parallel fracture model that will be repeatedly referred to throughout the thesis.

2.4.2 The governing equation for the porous matrix

The governing equation for the transport of the radionuclide through the porous matrix can be derived in a similar way. It is to be noted that the migration takes place along the x direction and there is no advective component. We consider a rectangle placed between $(x, x + \Delta x)$ and $(z, z + \Delta z)$ in the porous matrix. With this rectangle as a

base, one constructs an elementary parallelepiped of unit height with a volume of magnitude $(\Delta x \Delta z)$. Let C_p and S_p represent the dissolved and solid concentrations (both of them are expressed per unit volume) of the radioactive species within the porous matrix.

Then the amount of species present within this volume is given by

$$\left[\theta C_p \Delta x \Delta z + (1 - \theta) S_p \Delta x \Delta z \right]$$

The net addition due to diffusion is given by

$$\left[-\theta D_p \Delta z \frac{\partial}{\partial x} (C_p) \Big|_x + \theta D_p \Delta z \frac{\partial}{\partial x} (C_p) \Big|_{x+\Delta x} \right]$$

The decay of radioactive species per unit time within this volume is given by

$$\lambda \left[\theta C_p \Delta x \Delta z + (1 - \theta) S_p \Delta x \Delta z \right]$$

Then conservation of mass implies the following equation.

$$\begin{aligned} \frac{\partial}{\partial t} \left[\theta C_p \Delta x \Delta z + (1 - \theta) S_p \Delta x \Delta z \right] &= \left[-\theta D_p \Delta z \frac{\partial}{\partial x} (C_p) \Big|_x + \theta D_p \Delta z \frac{\partial}{\partial x} (C_p) \Big|_{x+\Delta x} \right] \\ &\quad - \lambda \left[\theta C_p \Delta x \Delta z + (1 - \theta) S_p \Delta x \Delta z \right] \end{aligned} \quad (2.10)$$

After simplification the above equation reduces to

$$\theta \frac{\partial C_p}{\partial t} + (1 - \theta) \frac{\partial S_p}{\partial t} = \theta D_p \frac{\partial^2 C_p}{\partial x^2} - \theta \lambda C_p - (1 - \theta) \lambda S_p \quad (2.11)$$

This is the pde governing the radionuclide transport through the porous matrix.

Rearranging the equation, one can write

$$\frac{\partial C_p}{\partial t} + \left(\frac{1 - \theta}{\theta} \right) \frac{\partial S_p}{\partial t} = D_p \frac{\partial^2 C_p}{\partial x^2} - \lambda C_p - \left(\frac{1 - \theta}{\theta} \right) \lambda S_p \quad (2.12)$$

Now like the fracture medium, we assume a linear relation between C_p and S_p .

$$S_p = k C_p \quad (2.13)$$

where k is a dimensionless quantity and it is related to the distribution coefficient of the porous matrix k_p in the following way.

$$k = k_p \rho_s \quad (2.14)$$

ρ_s is the true density of the porous matrix. We substitute eq. (2.13) and eq. (2.14) into eq. (2.12)

$$\left[1 + \frac{1-\theta}{\theta} k_p \rho_s \right] \frac{\partial C_p}{\partial t} = D_p \frac{\partial^2 C_p}{\partial x^2} - \left[1 + \frac{1-\theta}{\theta} k_p \rho_s \right] \lambda C_p \quad (2.15)$$

Now from the definition of porosity (θ), we can write

$$\theta = \frac{\text{Pore volume}}{\text{Pore volume} + \text{Solid volume}}; \quad (1-\theta) = \frac{\rho_b}{\rho_s} \quad (2.16)$$

where ρ_b is the bulk density of the porous matrix. If we substitute eq. (2.16) into eq. (2.15) we get

$$\left[1 + \rho_b \frac{k_p}{\theta} \right] \frac{\partial C_p}{\partial t} = D_p \frac{\partial^2 C_p}{\partial x^2} - \left[1 + \rho_b \frac{k_p}{\theta} \right] \lambda C_p \quad (2.17)$$

The retardation coefficient of the porous matrix R_p is defined as

$$R_p = 1 + \rho_b \frac{k_p}{\theta} \quad (2.18)$$

Rearranging eq. (2.17) we arrive at the final expression for the equation governing the transport through the porous matrix.

$$\frac{\partial C_p}{\partial t} - \frac{D_p}{R_p} \frac{\partial^2 C_p}{\partial x^2} + \lambda C_p = 0, \quad b \leq x \leq B, \quad t \geq 0 \quad (2.19)$$

The above equation [eq. (2.19)] along with eq. (2.9) form a set of coupled pde's that will be used throughout the remaining chapters.

The initial conditions for this set of coupled pde's are given by

$$C(z, 0) = 0 \quad , \quad z \geq 0 \quad (2.20)$$

$$C_p(x, z, 0) = 0 \quad , \quad b \leq x \leq B \quad , \quad z \geq 0 \quad (2.21)$$

$C(z, t)$ remains finite as $z \rightarrow \infty$. This leads to the following boundary condition.

$$C(\infty, t) = 0 \quad , \quad t \geq 0 \quad (2.22)$$

The mass conservation at the waste-fracture interface gives the following inlet boundary condition.

$$-D \left[\frac{\partial C}{\partial z} \right]_{z=0} + vC(0, t) = vC_0 \quad (2.23)$$

where C_0 is the concentration of the waste matrix. The molecular flux is continuous across the fracture-porous matrix interface and this leads to

$$C_p(b, z, t) = C(z, t) \quad , \quad z \geq 0 \quad , \quad t \geq 0 \quad (2.24)$$

The concentration profile C_p is symmetric around the line $x = B$ and this implies the following condition.

$$\left\{ \frac{\partial C_p}{\partial x} \right\}_{B, z, t} = 0 \quad , \quad z \geq 0 \quad , \quad t \geq 0 \quad (2.25)$$

With these initial, boundary and inlet conditions and assuming a source of constant strength ($C_0 = a$ constant), Chen and Li ^[7] provide an analytical solution based on a Laplace transformation that is given below. As we remarked earlier, it is a two dimensional integral that is not amenable to exact evaluation and hence needs a quadrature.

$$C(z, t) = \frac{2C_0}{\pi} \int_0^t d\xi (F_1 - F_2) \int_0^\infty F_3 [F_4 + F_5 F_6] d\varepsilon \quad (2.26)$$

All the terms of the above equation are defined below.

$$G = (R_p / D_p)^{(1/2)} ; \sigma = G(B - b) ; \alpha = \frac{v}{2D} ; \beta = \frac{(4RD)^{1/2}}{v} \quad (2.27)$$

$$A = \frac{bR}{\theta(D_p R_p)^{(1/2)}} ; \varepsilon_R = -\frac{\xi \varepsilon \sinh(\sigma \varepsilon) - \sin(\sigma \varepsilon)}{2A \cosh(\sigma \varepsilon) + \cos(\sigma \varepsilon)} \quad (2.28)$$

$$\Omega = \frac{\xi \varepsilon \sinh(\sigma \varepsilon) + \sin(\sigma \varepsilon)}{2A \cosh(\sigma \varepsilon) + \cos(\sigma \varepsilon)} \quad (2.29)$$

$$F_1 = \frac{1}{\beta \sqrt{\pi \xi}} \exp\left(-\frac{(z\alpha\beta)^2}{4\xi} - \xi(\beta^{-2} + \lambda) + z\alpha\right) \quad (2.30)$$

$$F_2(z, \alpha, \beta, \xi, \lambda) = \frac{1}{\beta^2} \exp(2z\alpha - \lambda\xi) \operatorname{Erfc}\left(\frac{z\alpha\beta}{2\sqrt{\xi}} + \frac{\sqrt{\xi}}{\beta}\right) \quad (2.31)$$

$$F_3(\varepsilon, \varepsilon_R, \lambda) = \frac{\varepsilon \exp(\varepsilon_R)}{\lambda^2 + (\varepsilon^4 / 4)} \quad (2.32)$$

$$F_4(\varepsilon, \Omega, \lambda) = (\varepsilon^2 / 2) \sin(\Omega) + \lambda \cos(\Omega) ; \varepsilon_I = (\varepsilon^2 t / 2) - \Omega \quad (2.33)$$

$$F_5(\lambda, t, \xi) = \exp[-\lambda(t - \xi)] ; F_6 = (\varepsilon^2 / 2) \sin(\varepsilon_I)_{t=t-\xi} - \lambda \cos(\varepsilon_I)_{t=t-\xi} \quad (2.34)$$

We list the typical values of the parameters that will be used throughout in our calculations.

$$D=1.0 (m^2 / yr) ; D_p=0.01 (m^2 / yr) ; R=1.0 ; R_p=1.0 ; v=1.0(m / yr) ; \\ T_{1/2}=2.14E+06 yr ; \lambda=\log(2)/T_{1/2} ; b=0.0005m ; \theta=0.01 ; B=1000m.$$

Here we need few comments regarding the oscillatory nature of the integrand.

The terms $\cos(\sigma\varepsilon)$ and $\sin(\sigma\varepsilon)$ introduce violent oscillations since the parameter σ can assume very large values. In addition, the z dependent quantities lead to exponential over flow and under flow for large z values. These factors limit the evaluation of the analytical solution to smaller distances.

2.5 The FTCS Approach

The exact solution given by the two dimensional integral eq. (2.26) is elegant but the highly oscillatory nature of its integrand poses formidable difficulties. Using a double precision accuracy, the maximum distance of evaluation is about $200m$ that can be marginally extended by using a quadruple precision. Realizing this limitation, Mohankumar and Auerbach ^[9] applied the simple and explicit FTCS finite difference scheme to evaluate numerically the solution of the coupled pde's of this parallel fracture model. Another advantage of this approach is the fact that both the time dependent and the time independent sources can be handled without restriction while the analytical solution presupposes a constant source. Let i and j denote the space and the time indices, respectively. Then C_i^j represents the concentration C at the time $j\Delta t$ and at the spatial point $i\Delta z$. Below we indicate the approximations for the different partial derivatives.

$$\frac{\partial C_i^j}{\partial t} \approx \frac{C_i^{j+1} - C_i^j}{\Delta t} \quad (2.35)$$

$$\frac{\partial C_i^j}{\partial z} \approx \frac{C_{i+1}^j - C_{i-1}^j}{2\Delta z} \quad (2.36)$$

$$\frac{\partial^2 C_i^j}{\partial z^2} \approx \frac{C_{i+1}^j - 2C_i^j + C_{i-1}^j}{(\Delta z)^2} \quad (2.37)$$

A similar discretization scheme is adopted for C_p too. In the FTCS scheme, the discretization error in the spatial derivatives is of the order of (Δz^2) while the error in the approximation of the time derivative is of the order of (Δt) . In the present problem, there is another important aspect which critically controls the accuracy of the results. The mass flux of the radionuclide entering into the fracture from the source is governed by the

concentration gradient $\left[\frac{\partial C}{\partial z} \right]_{z=0}$. Similarly, $\left[\frac{\partial C_p}{\partial x} \right]_{x=b}$ determines the mass flux across the fracture-porous matrix interface. Unless one evaluates these first order derivatives accurately, the concentration evaluations in both the z and x directions will be prone to error. The usual tendency is to approximate these derivatives by a 2 or 3 point formula but this order of derivative approximation is insufficient. As demonstrated by Mohankumar and Auerbach ^[9, 10], unless one employs a higher order like a 7th order derivative approximation, the concentrations at distances like 200m will be in error by about two orders. For equispaced grid points, the method of undetermined coefficients can be used to provide the required higher order derivative approximation. In the next section, we will outline this method.

2.6 The method of undetermined coefficients

In a finite difference approximation, the derivative is expressed as a linear combination of function values ^[11, 12]. Let z be the grid point where the derivative needs to be approximated. We consider the function values at $(m+n)$ points around z , (m points on the left and n points on the right of z). This gives a $(m+n+1)$ point derivative approximation that can be written in the following way.

$$\begin{aligned} \frac{df}{dz} \approx (1/h)[a_m f(z-mh) + a_{m-1} f(z-(m-1)h) + a_{m-2} f(z-(m-2)h) + \dots \\ + a_1 f(z-h) + a_0 f(z) + b_1 f(z+h) + b_2 f(z+2h) + \dots + b_n f(z+nh)] \end{aligned} \quad (2.38)$$

Here we need the values of a_i 's and b_i 's. To make the calculation simple, one can choose z as zero. Then setting $f(z)$ equal to $z^0, z, z^2, \dots, z^{m+n}$ in succession, the

derivative $\left[\frac{df}{dz} \right]$ can be evaluated at $z=0$ analytically. Then by setting this exact derivative equal to approximate value as given by the above formula, one gets a set of $(m+n+1)$ linear equations. The solution of these equations gives the values of all a_i 's and b_i 's. For example, a 7-point forward derivative approximation is given below.

$$\begin{aligned} \frac{df}{dz} \approx (1/h) \left(-\frac{49}{20} \right) f(z) + (1/h) (6) f(z+h) + (1/h) \left(-\frac{15}{2} \right) f(z+2h) + (1/h) \left(\frac{20}{3} \right) f(z+3h) \\ - (1/h) \left(\frac{15}{4} \right) f(z+4h) + (1/h) \left(\frac{6}{5} \right) f(z+5h) - (1/h) \left(\frac{1}{6} \right) f(z+6h) \end{aligned} \quad (2.39)$$

2.7 The CN approach

The FTCS scheme employed by Mohankumar et al. ^[9] is of first order accuracy in the time variable and is of second order accuracy in the space variable. Subsequently, to obtain a second order accuracy in both the space and time variables, Mohankumar ^[13] used the CN scheme. As in the earlier case, we denote the time and the space indices by j and i , respectively. Then in this scheme, the time and spatial derivatives are approximated in the following way.

$$\frac{\partial C_i^j}{\partial t} \approx \frac{C_i^{j+1} - C_i^j}{\Delta t} \quad (2.40)$$

$$\frac{\partial C_i^j}{\partial z} \approx (1/2) \left\{ \frac{C_{i+1}^j - C_{i-1}^j}{2\Delta z} + \frac{C_{i+1}^{j+1} - C_{i-1}^{j+1}}{2\Delta z} \right\} \quad (2.41)$$

$$\frac{\partial^2 C_i^j}{\partial z^2} \approx (1/2) \left\{ \frac{C_{i+1}^j - 2C_i^j + C_{i-1}^j}{(\Delta z)^2} + \frac{C_{i+1}^{j+1} - 2C_i^{j+1} + C_{i-1}^{j+1}}{(\Delta z)^2} \right\} \quad (2.42)$$

A similar discretization scheme is adopted for C_p also. Here, the spatial discretization is

centered at the time equal to $\left(j + \frac{1}{2}\right)\Delta t$. The approximations of the first and the second order spatial derivatives of the concentration are constructed to center around the same time quantity, $\left(j + \frac{1}{2}\right)\Delta t$ as indicated by eqs. (2.41, 2.42). With these discretizations, one gets a set of linear algebraic equations for the quantities C and C_p . The resulting linear equations for C supplemented with the interface conditions eq. (2.23) (approximated by a 7-point formula) have a band matrix structure while for C_p , the corresponding matrix is a tridiagonal one.

2.8 The DF Scheme

This is an explicit numerical scheme capable of second order accuracy in both the space and the time variables. Unlike the CN method, here all the derivatives are centered around the time $j\Delta t$. The main advantage of this scheme is that, it uses less memory space as compared to the CN method. Thus it is comparatively faster than the other implicit and semi-implicit schemes. Here the derivatives are approximated in the following way.

$$\frac{\partial C_i^j}{\partial t} \approx \frac{C_i^{j+1} - C_i^{j-1}}{2\Delta t} \quad (2.43)$$

$$\frac{\partial C_i^j}{\partial z} \approx \frac{C_{i+1}^j - C_{i-1}^j}{2\Delta z} \quad (2.44)$$

$$\frac{\partial^2 C_i^j}{\partial z^2} \approx \frac{C_{i+1}^j - C_i^{j+1} - C_i^{j-1} + C_{i-1}^j}{(\Delta z)^2} \quad (2.45)$$

As in the earlier cases, we approximate the interface derivatives by a 7-point forward

formula.

2.9 The higher order compact finite difference scheme

Till now we have discussed the schemes which are capable of providing second order accuracy in the space and the time domains. For our parallel fracture model, we need an assessment of the concentration for longer times and larger distances. As the value of z increases, the accuracy of the concentration values may deteriorate due to an error accumulation. Hence the need for more accurate schemes is felt. In fd approximations the derivatives can be subjected to higher order approximations (a five point central difference approximation is required for a fourth order accuracy). This has a major drawback. The first point just after the left boundary does not have sufficient number of grid points to its left for the desired degree of derivative approximation. A similar problem exists for the last point just before the right boundary. One may overcome these problems partially by introducing fictitious boundary points.

This was the motivation for a number of researchers to develop a higher order compact finite difference scheme that would use only three points to approximate the spatial derivative though the accuracy would be of higher order. For a hyperbolic equation, Kreiss et al. ^[14] were the first to report such a compact finite difference scheme that retained the tridiagonal form of the discretized equations with an accuracy of fourth order. Hirsh ^[15] followed the ideas of Kreiss et al. ^[14] to solve a parabolic equation namely, the Burger's equation in the following way.

$$y_n' = \left(\frac{D_0}{1 + \frac{1}{6}h^2 D_+ D_-} \right) y_n \quad (2.46)$$

$$y_n'' = \left(\frac{D_+ D_-}{1 + \frac{1}{12}h^2 D_+ D_-} \right) y_n \quad (2.47)$$

where $D_0 y_n = \left(\frac{1}{2h} \right) (y_{n+1} - y_{n-1})$, $D_+ y_n = \left(\frac{1}{h} \right) (y_{n+1} - y_n)$, $D_- y_n = \left(\frac{1}{h} \right) (y_n - y_{n-1})$ and

h is the mesh width. Now after rearranging we arrive at the following tridiagonal system of equations that can be easily solved by the Thomas algorithm.

$$\frac{1}{6} y_{n+1}' + \frac{2}{3} y_n' + \frac{1}{6} y_{n-1}' = \frac{1}{2h} (y_{n+1} - y_{n-1}) \quad (2.48)$$

$$\frac{1}{12} y_{n+1}'' + \frac{5}{6} y_n'' + \frac{1}{12} y_{n-1}'' = \frac{1}{h^2} (y_{n+1} - 2y_n + y_{n-1}) \quad (2.49)$$

Lele ^[16] reported a compact scheme that had a spectral like resolution. Sun and Zhang ^[17] implemented a method that was fourth-order accurate in both the space and the time variables to solve the heat equation. Cecchi and Pirozzi ^[18] reported a family of fully discrete finite difference implicit methods which could provide third order accuracy in the space variable and second order accuracy in the time domain. For our porous flow problem, we follow a version of a higher order compact fd scheme of Mohebbi and Dehghan ^[19]. This scheme is capable of providing results which are 4-th order accurate in the spatial domain. The higher order accuracy comes from the evaluation of the error terms (up to 4-th order) by a repeated differentiation of the original differential equation. For the sake of illustration, let us consider a second order differential equation with its boundary conditions in the domain $[0, l]$.

$$\alpha_1 \frac{d^2 y(x)}{dx^2} - \alpha_2 \frac{dy(x)}{dx} = g(x) \quad (2.50)$$

$$y(0) = y_0, \quad y(l) = y_l \quad (2.51)$$

We approximate the spatial derivatives by a central difference formula

$$\delta y = \frac{y_{i+1} - y_{i-1}}{2\Delta x} \quad (2.52)$$

$$\delta^2 y = \frac{y_{i+1} - 2y_i + y_{i-1}}{(\Delta x)^2} \quad (2.53)$$

By substituting these approximations into the original the differential equation, one gets a discretized expression as follows.

$$\alpha_1 \delta^2 y_i - \alpha_2 \delta y_i - \tau_i = g_i \quad (2.54)$$

where,

$$\tau_i = \frac{(\Delta x)^2}{12} \left(\alpha_1 \frac{d^4 y}{dx^4} - 2\alpha_2 \frac{d^3 y}{dx^3} \right) + O(\Delta x^4) \quad (2.55)$$

If we differentiate the original differential equation, we get

$$\left(\frac{d^3 y}{dx^3} \right)_i = \frac{1}{\alpha_1} \left(\frac{dg}{dx} + \alpha_2 \frac{d^2 y}{dx^2} \right) = \frac{1}{\alpha_1} (\delta g_i + \alpha_2 \delta^2 y_i) + O(\Delta x^2) \quad (2.56)$$

$$\left(\frac{d^4 y}{dx^4} \right)_i = \frac{1}{\alpha_1} \left(\frac{d^2 g}{dx^2} + \alpha_2 \frac{d^3 y}{dx^3} \right) = \frac{1}{\alpha_1} \delta^2 g_i + \frac{\alpha_2}{\alpha_1^2} \delta g_i + \frac{\alpha_2^2}{\alpha_1^2} \delta^2 y_i + O(\Delta x^2) \quad (2.57)$$

The final compact difference formula of fourth order accuracy can be written as

$$\left[\alpha_1 + \frac{\alpha_2 (\Delta x)^2}{12\alpha_1} \right] \delta^2 y_i - \alpha_2 \delta y_i = g_i + \frac{(\Delta x)^2}{12} \left(\delta^2 g_i - \frac{\alpha_2}{\alpha_1} \delta g_i \right) + O(\Delta x^4) \quad (2.58)$$

For the time discretization, we resort to a conventional CN like time approach by

centering the spatial variables around $\left(j + \frac{1}{2} \right) \Delta t$ and this gives a second order accuracy

in the time variable. Moreover, here also a 7-point formula is implemented to discretize the interface derivative.

2.10 The 4th order CN approach

The conventional CN scheme of second order accuracy in the space variable is modified to a yield fourth order accuracy in the spatial discretization. This is accomplished by replacing the second order spatial central differencing formula with a fourth order approximation. For the time discretization, there is no modification and hence we still have a second order accuracy. The required derivative approximations are indicated below.

$$\frac{\partial C_i^j}{\partial t} \approx \frac{C_i^{j+1} - C_i^j}{\Delta t} \quad (2.59)$$

$$\frac{\partial C_i^j}{\partial z} \approx (1/24) \left\{ \frac{-C_{i+2}^j + 8C_{i+1}^j - 8C_{i-1}^j + C_{i-2}^j}{\Delta z} + \frac{-C_{i+2}^{j+1} + 8C_{i+1}^{j+1} - 8C_{i-1}^{j+1} + C_{i-2}^{j+1}}{\Delta z} \right\} \quad (2.60)$$

$$\frac{\partial^2 C_i^j}{\partial z^2} \approx (1/24) \left\{ \frac{-C_{i+2}^j + 16C_{i+1}^j - 30C_i^j + 16C_{i-1}^j - C_{i-2}^j}{(\Delta z)^2} + \frac{-C_{i+2}^{j+1} + 16C_{i+1}^{j+1} - 30C_i^{j+1} + 16C_{i-1}^{j+1} - C_{i-2}^{j+1}}{(\Delta z)^2} \right\} \quad (2.61)$$

Though this scheme provides a fourth order accuracy in the space variable and a second order accuracy in the time part, it suffers from a limitation. The point just after the left boundary does not have enough grid points on the left side to implement this scheme. Similarly, the point just before the right boundary suffers from the same problem. There are two ways to overcome this limitation. One can introduce some fictitious grid points to implement this scheme. Otherwise some other scheme capable of providing the same

accuracy in both the space and the time variable is to be implemented only at these points. If any less accurate scheme (like the conventional CN scheme) is implemented at these points near the boundary, it will impair the overall accuracy of this higher order approximation. In the present problem, we implemented the HOCS (described in the previous section) at these two points as it can provide the required higher accuracy.

2.11 A stability analysis

In this section, the stability analysis of the finite difference schemes is discussed. Specifically, we restrict the analysis to the higher CN and HOC schemes using a Fourier stability method. First we discuss the analysis for the HOC scheme. For this, we consider the governing equations namely eq. (2.9) and eq. (2.19). Here, the source term of eq. (2.9) that gives a coupling between the fracture and the porous matrix is omitted for simplicity and hence we analyze the following equation.

$$\frac{\partial C}{\partial t} + \frac{v}{R} \frac{\partial C}{\partial z} - \frac{D}{R} \frac{\partial^2 C}{\partial z^2} + \lambda C = 0 \quad (2.62)$$

Let Δz be the mesh width along the z axis and Δt is the time step. We indicate the space and the time indices by n and j , respectively. Then upon discretization using the HOC scheme, the above equation takes the following form.

$$\begin{aligned} & \left(\frac{S_4 - S_5}{2} - \frac{S_6 + 1/12}{\Delta t} \right) C_{n-1}^{j+1} - \left(\frac{2S_4 + \lambda}{2} + \frac{5}{6\Delta t} \right) C_n^{j+1} + \left(\frac{S_4 + S_5}{2} + \frac{S_6 - 1/12}{\Delta t} \right) C_{n+1}^{j+1} \\ & = - \left(\frac{S_4 - S_5}{2} + \frac{S_6 + 1/12}{\Delta t} \right) C_{n-1}^j + \left(\frac{2S_4 + \lambda}{2} - \frac{5}{6\Delta t} \right) C_n^j - \left(\frac{S_4 + S_5}{2} - \frac{S_6 - 1/12}{\Delta t} \right) C_{n+1}^j \end{aligned} \quad (2.63)$$

The various terms of eq. (2.63) are listed below.

$$S_4 = \frac{D}{R(\Delta z)^2} + \frac{v^2}{12DR} - \frac{\lambda}{12} ; S_5 = \frac{\lambda v(\Delta z)}{24D} - \frac{v}{2(\Delta z)R} ; S_6 = \frac{v(\Delta z)}{D} \quad (2.64)$$

For a Fourier stability analysis, we set

$$C_n^j = (\rho_f)^j \exp(ikn\Delta z) \quad (2.65)$$

where k is the wave number and ρ_f is the error amplification factor for the fracture.

Substituting this in eq. (2.63) and setting $k\Delta z = \theta_f$, we get

$$|\rho_f|^2 = \frac{\left[S_4 \cos(\theta_f) + \frac{1}{6\Delta t} \cos(\theta_f) + S_4 + \frac{\lambda}{2} - \frac{5}{6\Delta t} \right]^2 + \left[S_5 \sin(\theta_f) - \frac{2}{\Delta t} S_6 \sin(\theta_f) \right]^2}{\left[S_4 \cos(\theta_f) + \frac{1}{6\Delta t} \cos(\theta_f) - S_4 - \frac{\lambda}{2} - \frac{5}{6\Delta t} \right]^2 + \left[S_5 \sin(\theta_f) + \frac{2}{\Delta t} S_6 \sin(\theta_f) \right]^2} \quad (2.66)$$

For stability, one should have $|\rho_f|^2 \leq 1$. For our analysis, since we need an equation, we set $|\rho_f|^2 = 1$. This gives the following equation.

$$\begin{aligned} & \left[S_4 \cos(\theta_f) + \frac{1}{6\Delta t} \cos(\theta_f) + S_4 + \frac{\lambda}{2} - \frac{5}{6\Delta t} \right]^2 + \left[S_5 \sin(\theta_f) - \frac{2}{\Delta t} S_6 \sin(\theta_f) \right]^2 \\ & - \left[S_4 \cos(\theta_f) + \frac{1}{6\Delta t} \cos(\theta_f) - S_4 - \frac{\lambda}{2} - \frac{5}{6\Delta t} \right]^2 - \left[S_5 \sin(\theta_f) + \frac{2}{\Delta t} S_6 \sin(\theta_f) \right]^2 = 0 \quad (2.67) \end{aligned}$$

With a known value of Δz , we need to find a value of Δt that satisfies the above equation.

Since the wave number and hence θ_f are unknown, we need to get another equation that involves θ_f and Δt . This required equation is obtained by demanding that we maximize Δt with respect to θ_f . This gives the following equation.

$$\frac{\partial(\Delta t)}{\partial\theta_f} = \frac{\left(\frac{5}{36}\right)\sin(\theta_f) - \left(\frac{v^2\Delta t}{36R^2}\right)\sin(\theta_f)\cos(\theta_f) + \left[\frac{v^4(\Delta t)^2}{144R^2}\right]\sin(\theta_f)}{\left(\frac{5v^2}{72R^2}\right) - \left(\frac{v^2}{72R^2}\right)\cos^2(\theta_f) - \left[\frac{v^4(\Delta t)^2}{72R^4}\right]\cos(\theta_f)} = 0 \quad (2.68)$$

Eq. (2.67) and eq. (2.68) need to be solved in tandem using the Newton-Raphson technique, to get the required value of time step, Δt . One needs to check by a second derivative condition that the time step value obtained is indeed a maxima and not a minima.

At this stage, one knows the values of Δz and Δt . For the stability analysis of the porous matrix equation, we set up two equations similar to eq. (2.66) and eq.(2.67) that involve the quantities, ρ_p and θ_p , the amplification factor and the wave number related quantity for the porous side, respectively. Repeating the earlier steps, we evaluate θ_p and Δx . Hence we have the required quantities, namely Δt and Δx for a given Δz that will guarantee a stability. But as we see the above method is too complicated if not impossible.

So here we indicate a practical approach to fix the required quantities. First we fix a value for Δz . As the migration through a fracture is dominated by an advection, we use the Courant-Friedrichs-Lewy (CFL) condition ^[20] to get an estimate of Δt . Let us call the time step that is obtained as Δt_l . On the other hand, the migration of the radionuclide through a porous matrix is dominated by a diffusion process. Here the mesh width Δx must be greater than the diffusion length corresponding to a time step Δt . To ensure stability one can choose Δt in such way that Δx is a multiple of the diffusion length. For

our purpose, we have chosen Δx as six times the diffusion length. Let us call the Δt corresponding to this as Δt_2 . Now for an overall stability, we choose the minimum of Δt_1 and Δt_2 as the required time step. The stability analysis for the higher order CN method also has a similar complexity and hence the practical procedure that we have just now outlined is once again followed.

2.12 Result and discussions

All the reported calculations in this thesis are performed using an Intel Pentium Core (TM)2 Quad CPU Q 6600 PC with a clock speed 2.4 GHz and with a 3.23 GB RAM employing a Lahey Fortran compiler running under a Windows XP operating system. By employing a quadruple precision, the integral evaluation based reference analytical solution is calculated up to a distance of 200m. Beyond this distance, the non availability of reference values is indicated by dashes in the table. In table 2.4, the double precision results of the 2nd and the 4th order CN schemes, the DF scheme and the higher order compact (HOC) scheme are presented for a time period of 1000 yrs. The concentration values for these four schemes in a given row are followed by their absolute relative percentage errors that are given within brackets in the next row. Since the reference analytical values are available only up to 200m, these relative errors are also indicated up to the same distance. Unlike the analytical solution, the finite difference based evaluation is not limited by a distance factor. However, memory based restriction relating to the total number of grid points in both the z and the x directions will ultimately limit the maximum distance of evaluation for these fd schemes.

Let NX and NZ denote the number of grid points along the x and the z axis, respectively. Since the CN, the 4th order CN and the HOC schemes need matrix inversion, the maximum values that we can choose for NX and NZ are 5600 and 2800, respectively. The corresponding time step is $\Delta t = 0.02\text{yr}$. These three schemes need a run time of about 12 hrs. Since the DF scheme is an explicit one, we can set $NX=10,000$ and $NZ=8000$ with a time step of $\Delta t = 0.004\text{yr}$ and this method requires a run time of 80 hrs.

The foremost conclusion that can be drawn from the results is the fact that the 4th order CN and the HOC schemes offer relatively the best accuracy and they are comparable. This is followed by the accuracy of the CN scheme of second order. The DF scheme has the least accuracy even though theoretically its errors in both the time and space variables are of second order. In fact, the accuracy of the DF scheme is less than that of the 4th order CN and the HOC schemes by about three orders. Also, as the distance increases, the accumulation of error has its impact on all these schemes. The relative error of the CN scheme of second order is more by about one or two orders when compared to the errors of the 4th order CN and the HOC schemes. This is to be expected since the last two schemes have a fourth order error in the space variable. Hence we can choose either the 4th order CN scheme or the HOC scheme for the reliable assessment of the radionuclide concentration up to a distance of about 500m.

2.13 Conclusions

We have indicated that both the 4th order CN and the HOC schemes can be utilized for a reliable assessment of the radionuclide buildup for the deterministic parallel

fracture model. We have extended the maximum distance of evaluation of the analytical schemes which is about $200m$ to about $500m$ by employing these fd schemes. This is of practical interest since one needs a realistic assessment over such longer distances. Also, these approaches can handle both the time dependent and the time independent sources without restriction. It must be highlighted that the use of these two higher order schemes with the higher order interface derivatives is a first of its kind for this problem.

Table 2.1: Experimental values of the pore diffusivities (D_p)^[8]

Depth (m)	Iodine $D_p \times 10^{12} m^2/s$	Uranium $D_p \times 10^{12} m^2/s$
1.49	90	8
2.63	200	9
2.83	200	3
2.83	200	10

Table 2.2: Typical experimental values of pore diffusivity (D_p) and hydraulic conductivity (K_p) at different depths ^[8]

Depth (m)	$D_p \times 10^{10}$ m ² /s	$K_p \times 10^{13}$ m/s
0.36-0.48	> 1	> 2-5
0.78-1.41	0.5	0.1
1.46-1.59	0.05	< 0.1
1.74-2.24	1	1
2.62-2.67	> 1	> 2-5

Table 2.3: Typical pore size values ^[8]

Depth (m)	Porosity (in percentage)
2.575	0.21
0.555	0.47
1.825	0.42
0.825	0.42
1.315	0.36

Table 2.4: The concentration values and the relative percentage errors at different distances by different methods

Z (m)	Exact	CN ($\Delta t = 0.02\text{yr}$)	DF ($\Delta t = 0.004\text{yr}$)	HOC ($\Delta t = 0.02\text{yr}$)	4th CN ($\Delta t = 0.02\text{yr}$)
10	0.6293E+00	0.6293E+00 (0.298E-02)	0.6318E+00 (0.399E+00)	0.6293E+00 (0.432E-03)	0.6293E+00 (0.432E-03)
20	0.3627E+00	0.3627E+00 (0.735E-03)	0.3643E+00 (0.442E+00)	0.3628E+00 (0.639E-03)	0.3627E+00 (0.637E-03)
30	0.1841E+00	0.1841E+00 (0.145E-01)	0.1851E+00 (0.520E+00)	0.1842E+00 (0.154E-03)	0.1841E+00 (0.147E-03)
40	0.8219E-01	0.8224E-01 (0.529E-01)	0.8274E-01 (0.659E+00)	0.8220E-01 (0.165E-02)	0.8220E-01 (0.166E-02)
50	0.3230E-01	0.3234E-01 (0.126E+00)	0.3291E-01 (0.189E+02)	0.3231E-01 (0.549E-02)	0.3231E-01 (0.549E-02)
60	0.1119E-01	0.1122E-01 (0.246E+00)	0.1146E-01 (0.235E+02)	0.1120E-01 (0.122E-01)	0.1120E-01 (0.121E-01)
70	0.3427E-02	0.3441E-02 (0.426E+00)	0.3527E-02 (0.294E+02)	0.3427E-02 (0.225E-01)	0.3427E-02 (0.223E-01)
80	0.9290E-03	0.9353E-03 (0.681E+00)	0.9631E-03 (0.367E+02)	0.9293E-03 (0.373E-01)	0.9293E-03 (0.370E-01)
90	0.2236E-03	0.2259E-03 0.102E+01	0.2373E-03 (0.613E+02)	0.2237E-03 (0.576E-01)	0.2237E-03 (0.570E-01)

(Table 2.4 is continued in the next page)

100	0.4788E-04	0.4858E-04 (0.147E+01)	0.5140E-04 (0.735E+02)	0.4792E-04 (0.842E-01)	0.4792E-04 (0.833E-01)
200	0.2574E-13	0.2948E-13 (0.157E+02)	0.3644E-13 (0.431E+03)	0.2572E-13 (0.970E+00)	0.2571E-13 (0.959E+00)
300	0.1490E-26	0.2360E-26	0.9051E-27	0.9052E-27
400	0.2259E-43	0.4338E-43	0.6651E-44	0.6674E-44
500	0.3491E-63	0.5350E-63	0.3132E-64	0.3179E-64

2.14 References

- [1] I. Neretnieks, *J. Geophys. Res.* 85 (1980) 4379.
- [2] G.E. Grisak and J.F. Pickens, *Water Resour. Res.* 16 (1980) 719.
- [3] D.H. Tang, E.O. Frind and E.A. Sudicky, *Water Resour. Res.* 17 (1981) 555.
- [4] A. Rasmuson and I. Neretnieks, *J. Geophys. Res.* 86 (1981) 3749.
- [5] A. Rasmuson, *Water Resour. Res.* 20 (1984) 1435.
- [6] E.A. Sudicky and E.O. Frind, *Water Resour. Res.* 18 (1982) 1634.
- [7] C. T. Chen and S. H. Li, *Waste Manage.* 17 (1997) 53.
- [8] L. Birgersson and I. Neretnieks, *Water Resour. Res.* 26 (1990) 2833.
- [9] N. Mohankumar and S. M. Auerbach, *Comput. Phys. Commun.* 161 (2004) 109.
- [10] N. Mohankumar and S. M. Auerbach, *Comput. Phys. Commun.* 179 (2008) 773.
- [11] H.M. Antia, *Numerical Methods for Scientists and Engineers*, Tata McGraw-Hill, New Delhi, 1991.
- [12] C. Pozrikidis, *Numerical Computation in Science and Engineering*, Oxford University Press, New York, 1998.
- [13] N. Mohankumar, *Ann. Nucl. Energy* 34 (2007) 222.
- [14] H. O. Kreiss, S. A. Orszag, and M. Israeli, *Annu. Rev. Fluid Mech.* 6 (1974) 281.
- [15] R. S. Hirsh, *J. Comput. Phys.* 19 (1975) 90.
- [16] S. K. Lele, *J. Comput. Phys.* 103 (1992) 16.
- [17] H. Sun and J. Zhang, *Numer. Methods Partial Differ. Eq.* 19 (2003) 846.

[18] M.M. Cecchi and M.A. Pirozzi, *Appl. Numer. Math.* 55 (2005) 334.

[19] A. Mohebbi and M. Dehghan, *Appl. Math. Modell.* 34 (2010) 3071.

[20] E. Isaacson and H.B. Keller, *Analysis of Numerical Methods*, Dover, New York, 1994.

Chapter 3

Pseudospectral solution of the deterministic parallel fracture model

3.1 Introduction

3.2 A brief survey of literature

3.3 The equations for radioactivity migration in a porous medium

3.4 The pseudospectral method

3.4.1 The Chebyshev pseudospectral method

3.4.2 The Legendre pseudospectral method

3.5 Remarks on stability analysis

3.6 Results and discussion

3.7 Conclusions

3.8 References

3.1 Introduction

This chapter deals with a pseudospectral solution of the deterministic porous flow problem. For the parallel fracture model, the Laplace transform method provides an analytical solution in closed form only if the source is of constant strength. Also, the resulting solution in the form of a two dimensional integral contains a very highly oscillatory integrand and its evaluation for larger distances and longer times poses serious computational problems. We are interested in seeking numerical solutions that demand minimum computational cost but at the same time they must be capable of better accuracy for longer times and larger distances. With these objectives, in the preceding chapter, the pde's of the parallel fracture model were solved by a variety of finite difference methods. By these approaches, one can get concentrations up to a distance of about $500m$ with a reasonable accuracy and also, one is not constrained by a constant source requirement. This distance up to which the concentration is evaluated can be extended further by foregoing a bit of accuracy (by choosing a larger grid size). This is definitely *a significant improvement* since by resorting to a quadrature, the closed form solution can be evaluated only up to a maximum distance of about $200m$ in quadruple precision. But still the accuracy of these finite difference methods that we employ is of fourth order in the space variable and second order in the time variable. This raises a natural question as to whether more accurate methods can be adopted. The pseudospectral methods provide an affirmative answer to this question. They *provide very accurate results with minimum computational cost* even though the maximum distance at which the concentration can be evaluated is *not as large as in the case of the finite difference methods*.

The relatively poor accuracy of the finite difference methods stems from the fact that this process can be viewed as an approximation by a sequence of overlapping polynomials of low order that are used to interpolate the function at the grid points. One can enhance the accuracy by using a finer grid but this comes with an ever increasing computational cost. If the domain under consideration is very large as it happens in our parallel fracture model, the number of grid points increases in direct proportion. Also, for the porous problem one needs a fine grid in a two dimensional domain and this results in a large number of grid points and this in turn results in a large run time. Typically, the implicit schemes that are reported in the previous chapter demand an execution time of about *12hrs* and the memory related requirements are very excessive. The pseudospectral method circumvents these complications of the fd schemes by some ingenious ingredients. This method can be viewed as a *very high order polynomial approximation over the entire domain* that leads to its characteristic *exponential convergence*. As a result, one needs a lesser number of grid points that results in a much reduced computational cost and execution times. Hence for the porous problem, the pseudospectral method outperforms the fd methods. We will consider two variants of this approach, namely the Chebyshev and the Legendre methods for the solution of the radioactivity migration problem.

3.2 A brief survey of literature

In the pseudospectral method the unknown to be found is approximated as a sum of functions that belong to a complete set of basis functions. The infinite summation involving the basis functions is truncated for practical considerations. Let

function $u(x)$ be a solution of an one dimensional problem. In the pseudospectral approach, $u(x)$ is approximated as

$$u(x) \approx \sum_j a_j \theta_j(x) \quad (3.1)$$

Here $\theta_j(x)$ is a known function that belongs to a basis set. The problem of finding $u(x)$ now gets recast as a problem of fixing the coefficients $\{a_j\}$. In the pseudospectral scheme, one substitutes the above series in the equation to be solved and then demands the equality of the rhs and the lhs on a set of points that belong to the domain of $u(x)$. These points are called the collocation points. This collocation process provides as many equations as the number of unknowns $\{a_j\}$ that need to be found. By solving these resulting equations, one evaluates $\{a_j\}$ and hence finally the value of $u(x)$.

If the unknown function obeys periodic boundary conditions, then the choice of basis function naturally reduces to the trigonometric functions and the resulting pseudospectral method is called the Sinc or the Fourier pseudospectral method. If one chooses a polynomial basis set like the Chebyshev or the Legendre or the Laguerre basis functions, then one can evaluate an unknown function that obeys a non periodic boundary condition. In this case, $\theta_j(x)$ represents a basis polynomial of order j . Since our solution is not periodic, we use both the Chebyshev and Legendre basis functions and then compare their relative merits. In the following section a brief survey of the literature dealing with the pseudospectral method is presented.

Kreiss et al. ^[1] were the first to employ this pseudospectral strategy to the solution of a hyperbolic equation. This was later followed up by Fornberg ^[2]. Funaro and Gottlieb ^[3-4] used these ideas for the time dependent hyperbolic equations. Boyd ^[5] made a detailed analysis of different types of pseudospectral methods. In particular, he highlighted the role of non uniform grid points that were suitable when the equation to be solved had singularities. This was illustrated in the case of the Runge phenomenon. Boyd also developed ^[6] a fast algorithm for the Chebyshev, the Fourier and the Sinc interpolation. He also developed algorithms employing a modified Euler summation for a convergence acceleration on non uniform grids ^[7-8].

Don and Gottlieb ^[9] proposed an interesting method known as the Chebyshev-Legendre method. In their work, the Legendre polynomial was chosen as the basis function but the interpolation nodes were chosen as the Chebyshev-Gauss-Lobatto points which are the nodes of the Chebyshev pseudospectral method. This recipe was used for the solution of some parabolic and hyperbolic equations. This strategy exploits the advantages inherent to *both* the Legendre and Chebyshev methods. Later on this approach was extended to the solution of the elliptic equations ^[10]. This method was also utilized for solving the equations of non linear conservative laws ^[11], ^[12] and Kdv equations ^[13].

Merrill ^[14] made a detailed comparison of the finite difference approximation and the pseudospectral method for the shallow water equations in spherical coordinates. Ross and Fahroo ^[15] used the Legendre basis to address an optimal

control problem. Dehghan and Shamsi ^[16] solved a two-dimensional parabolic equation with a non standard boundary condition. Guo and Wang ^[17] proposed a modified version of the Laguerre pseudospectral method which was further refined by multi domain Legendre pseudospectral approximation. Javidi and Golbabai ^[18] reported a method to solve a parabolic partial differential equation with Neumann boundary condition. They used the Chebyshev polynomials as the basis set. This was extended to solve a non linear Schrodinger equation ^[19]. Here they used a numerical technique called preconditioning to minimize the round off errors. Golbabai and Javidi ^[20] also handled the non classical parabolic problems by this methodology. Akinpelu et al. ^[21] reported an interesting observation that there could be instances where the Legendre collocation method might prove superior to its Chebyshev counterpart.

3.3 The equations for the radioactivity migration in a porous medium

For the sake of convenience, the pde's that govern the migration of the radioactivity and the values of the parameters of the pde's are given below. All the details can be found in the previous chapter.

$$\frac{\partial C}{\partial t} + \frac{v}{R} \frac{\partial C}{\partial z} - \frac{D}{R} \frac{\partial^2 C}{\partial z^2} + \lambda C - \frac{\theta D_p}{Rb} \left[\frac{\partial C_p}{\partial x} \right]_{x=b} = 0 \quad (3.2)$$

$$\frac{\partial C_p}{\partial t} - \frac{D_p}{R_p} \frac{\partial^2 C_p}{\partial x^2} + \lambda C_p = 0 \quad (3.3)$$

$$D=1.0 (m^2 / yr) ; D_p=0.01 (m^2 / yr) ; R=1.0 ; R_p=1.0 ; v=1.0(m / yr) ; \\ T_{1/2}=2.14E+06 yr ; \lambda=log(2)/T_{1/2} ; b=0.0005 m ; \theta=0.01 ; B=1000 m.$$

3.4 The pseudospectral (PS) method

Let us assume that $u(x)$, the unknown function to be solved is defined on the interval $[-1, 1]$. We approximate the function by a polynomial $u_M(x)$ of degree at most M .

$$u_M(x) \approx \sum_{j=0}^M l_j(x) u(x_j) \quad (3.4)$$

The collocation requirement demands that $u(x)$ and $u_M(x)$ are equal on a set of collocation points $\{x_0, x_1, \dots, x_M\}$. This demands the following discrete orthogonality relation.

$$l_j(x_k) = \delta_{jk} ; j, k = 0, 1, \dots, M \quad (3.5)$$

Then one can write the n -th order derivative of $u(x)$ as ^[22].

$$u_M^n(x) = \sum_{j=0}^M l_j^n(x) u(x_j) \quad (3.6)$$

We express the above equation in matrix form in the following way.

$$U^n = F^n U \quad (3.7)$$

$$U^n = [U_M^n(x_0), U_M^n(x_1), \dots, U_M^n(x_m)]^T \quad (3.8)$$

$$U = [U(x_0), U(x_1), \dots, U(x_m)]^T \quad (3.9)$$

3.4.1 The Chebyshev pseudospectral method

In this method, the Chebyshev-Gauss-Lobatto points are taken as the collocation points. They are given by the following *explicit* relation.

$$x_j = \cos\left(\frac{j\pi}{M}\right) ; j = 0, \dots, M \quad (3.10)$$

The interpolating polynomial, $l_j(x)$ is expressed in terms of the M -th order Chebyshev polynomial $T_M(x)$ as follows ^[18].

$$l_j(x) = \frac{(-1)^{j+1}(1-x^2)T'_M(x)}{c_j M^2(x-x_j)} ; j = 0, 1, \dots, M \quad (3.11)$$

$$c_0 = c_M = 2 ; c_j = 1 ; j = 1, 2, \dots, M-1 \quad (3.12)$$

Now f_{kj} , the elements of the derivative matrix F are given by

$$f_{kj} = \begin{cases} -\frac{c_k}{2c_j} \frac{(-1)^{j+k}}{\sin\left[(k+j)\frac{\pi}{2M}\right] \sin\left[(k-j)\frac{\pi}{2M}\right]} ; k \neq j \\ -\frac{1}{2} \cos\left(\frac{k\pi}{M}\right) \left[1 + \cot^2\left(\frac{k\pi}{M}\right)\right] ; k = j ; k \neq 0, M \\ f_{00} = -f_{MM} = \frac{1+2M^2}{6} \end{cases} \quad (3.14)$$

3.4.2 The Legendre pseudospectral method

For this method, the Legendre-Gauss-Lobatto (LGL) nodes are taken as the collocation points $\{x_0, x_1, \dots, x_M\}$ with $x_0 = -1$ and $x_M = 1$. The remaining collocation

points are the zeros of $P'_M(x)$ which is the first derivative of the Legendre polynomial $P_M(x)$. There is no explicit formula for LGL nodes but they can be calculated numerically ^[15]. The interpolating polynomial, $l_j(x)$ expressed in terms of the M -th order Legendre polynomial $P_M(x)$ ^[16] is given below.

$$l_j(x) = \frac{(x^2 - 1)P'_M(x)}{M(M+1)P_M(x_j)(x - x_j)} ; j = 0, 1, \dots, M \quad (3.15)$$

The elements of F are given by

$$f_{kj} = \begin{cases} \frac{P_M(x_k) - 1}{P_M(x_j)(x_k - x_j)} & ; k \neq j \\ -\frac{M(M+1)}{4} & ; k = j = 0 \\ \frac{M(M+1)}{4} & ; k = j = M \\ 0 & ; \text{Otherwise} \end{cases} \quad (3.16)$$

Up to now for reasons of notational simplicity, u is assumed to depend only on x , the space variable. In case the unknown is a function of both the space and the time variables, one replaces $u_M(x)$ by $u_M(x, t)$ as follows.

$$u_M(x, t) = \sum_{j=0}^M l_j(x) u(x_j, t) \quad (3.17)$$

Now at a particular instant of time, all the spatial derivatives can be evaluated by any one of the schemes that we have just discussed. Once this is done, a forward difference formula can be utilized to calculate the value of $u(x, t)$ at the next instance of time. For example, consider the following differential equation.

$$\frac{\partial u}{\partial t} - \frac{\partial^2 u}{\partial x^2} + u = 0 ; \quad -1 \leq x \leq 1 ; \quad t \geq 0 \quad (3.18)$$

Let i and j denote the space and the time related indices, respectively. Then if one applies the pseudospectral approximation for the spatial domain and a forward difference formula for the time part, the above equation is discretized in the following way.

$$\frac{u_i^{j+1} - u_i^j}{\Delta t} - \sum_{k=0}^M f_{ik}^2 u_k^j + u_i^j = 0 \quad (3.19)$$

As all the u_i^j s are known, one can find u_i^{j+1} .

3.5 Remarks on stability analysis

The stability analysis for this set of coupled pde's is very complicated. This will be pursued as a future work as a sequel to this thesis. Presently, we fix the time step by numerical experimentation. Let us assume that we have chosen a time step Δt . Next we evaluate the concentrations with a time step $\Delta t/2$. If the results are nearly the same, we conclude that the results do not diverge. The concentration values corresponding to $\Delta t/2$ are taken as a solution.

3.6 Results and discussion

Here we present the numerical results of the parallel fracture model employing both the Chebyshev and the Legendre pseudospectral schemes. The calculations of table 3.1 and table 3.2 are performed for a time of *1000 yrs*. For both the methods, the

number of basis functions (equal to the number of grid points) chosen is the same and this is maintained for approximation along both the z and x directions. Let NZ and NX be the number of grid points along the z and x axes, respectively. For the present calculation, the values employed are $NZ=101$ and $NX=201$ with a time step value, $\Delta t = 0.02yr$. In Table 3.1, the concentration values calculated by these two methods in quadruple precision are given. As we saw in the previous chapter, the higher order CN and the higher order compact fd give the best results among the schemes compared. But it must be noted that the higher order CN method is computationally relatively more involved since one needs to solve pentadiagonal matrices whereas the higher order compact fd scheme needs only the solution of a simpler tridiagonal matrix. Hence for our comparison purposes, the results of our pseudospectral schemes are compared with that of the higher order compact fd scheme. The number of grid points along the z and x directions for the higher order compact fd scheme are 2800 and 5600 respectively.

The relative percentage errors of all the schemes in double precision accuracy are tabulated in table 3.2. It can be easily seen that *the errors obtained from the two pseudospectral schemes are much less compared to the results of their fd counterpart*. There is one more huge gain the psedospectral methods enjoy over the higher order compact fd scheme. Both the Chebyshev and Legendre methods need a run time of about 10 min. This must be contrasted with the run time of about 12 hrs needed by the present fd scheme. This implies *a reduction in computing time by a factor 72*. Also, this much reduced computing time comes with a much diminished computer memory requirement since the pseudospectral methods needs only a 101 by 201 grid while the

fd scheme needs a 2800 by 5600 grid. Thus the total number of grid points is reduced by a factor of about 772 for the pseudospectral methods. These facts establish the pseudospectral method as a superior candidate when compared to its fd counterpart.

Some elaboration is needed regarding the maximum distance at which the concentration by the pseudospectral method can be evaluated. If C_0 is the original concentration then roughly $C_0 10^{-16}$ is the *smallest concentration value* that can be estimated by the pseudospectral approach in double precision. For our chosen model problem, the drop in the concentration by an order of magnitude 16 happens when the z value is about $200m$. This sets an upper limit on the maximum distance of evaluation. This distance can be increased to about $300m$ by resorting to quadruple precision. It must be remembered that the finite difference methods do not suffer from these restrictions. However the memory related restrictions define the smallest grid one can choose and this in turn restricts the largest distance of evaluation for the fd schemes.

The results indicated in tables (3.1, 3.2) show that both the Legendre and Chebyshev are accurate and comparable. However, for our porous flow case, the Legendre scheme gives mildly more accurate results at shorter distances. However, it must be kept in mind that the node evaluation for the Legendre scheme needs a little bit of extra computation since the nodes are *not* explicitly given. On the other hand, the nodes of the Chebyshev scheme involve a simple and explicit algebraic formula. Finally, the entries in the second column of table 3.1 are the exact values obtained by

the integral evaluation [eq. (2.26)] that are available only up to a distance of $200m$. Hence beyond this distance the second column carries no entries.

In table 3.3, we indicate the concentration profiles calculated by the Chebyshev pseudospectral and the HOC scheme for a time of 100 yrs in double precision. The corresponding relative percentage errors are given in the brackets. For these calculations, the flow velocity of water through a fracture is taken as $4m/yr$. All other rock related parameters are kept unchanged. Here, we use a time step (Δt) of $0.02yr$ for the HOC scheme. For the Chebyshev pseudospectral method, we choose $\Delta t = 0.001yr$.

3.7 Conclusions

In summary, the conclusions that can be drawn from the combined results of this and the previous chapters are as follows. If the distance of evaluation is less than $300m$, then either the Legendre or the Chebyshev pseudospectral method is the method of choice. They offer exponential convergence at much reduced computational cost. If the distance exceeds $300m$, then for these larger distances, the higher order compact fd scheme and the higher order CN scheme are preferable and among these two methods the former one is a better candidate. The combination of these *two sets of methods provide us with reliable algorithms* by which one can accurately assess the concentration of radioactivity migration without any ambiguity by the deterministic routes. Compared to the higher order fd methods, for the pseudospectral method the run time gets reduced by a factor 72 while the memory

requirements get reduced by a factor 772. These gains are very impressive. Finally, it must be noted that *the application of the pseudospectral methods for the radioactivity migration was done for the first time in these investigations.*

Table 3.1: Comparison of the concentration values calculated by the two pseudospectral methods ($\Delta t=0.02$ yr)

(Calculations are performed in quadruple precision)

Z (metre)	Exact	Legendre pseudospectral	Chebyshev pseudospectral
10	0.6293E+00	0.6293E+00	0.6293E+00
20	0.3627E+00	0.3627E+00	0.3627E+00
30	0.1841E+00	0.1841E+00	0.1841E+00
40	0.8219E-01	0.8219E-01	0.8219E-01
50	0.3230E-01	0.3230E-01	0.3230E-01
60	0.1119E-01	0.1119E-01	0.1119E-01
70	0.3427E-02	0.3426E-02	0.3426E-02
80	0.9290E-03	0.9289E-03	0.9289E-03
90	0.2236E-03	0.2235E-03	0.2235E-03

(Table 3.1 is continued in the next page)

100	0.4788E-04	0.4787E-04	0.4787E-04
120	0.1562E-05	0.1561E-05	0.1561E-05
140	0.3283E-07	0.3281E-07	0.3281E-07
160	0.4520E-09	0.4515E-09	0.4515E-09
180	0.4135E-11	0.4128E-11	0.4128E-11
200	0.2547E-13	0.2540E-13	0.2540E-13
220	0.1065E-15	0.1065E-15
240	0.3072E-18	0.3072E-18
260	0.6156E-21	0.6156E-21
280	0.8647E-24	0.8647E-24
300	0.8552E-27	0.8535E-27

Table 3.2: Relative percentage errors of different methods ($\Delta t = 0.02 \text{ yr}$)

(Calculations are performed in double precision)

Z (meter)	Legendre pseudospectral Err.	Chebyshev pseudospectral Err.	HOCS Err.
10	0.166E-03	0.173E-03	0.432E-03
20	0.277E-03	0.294E-03	0.639E-03
30	0.259E-03	0.275E-03	0.154E-03
40	0.107E-04	0.385E-04	0.165E-02
50	0.864E-03	0.873E-03	0.549E-02
60	0.242E-02	0.242E-02	0.122E-01
70	0.494E-02	0.494E-02	0.225E-01
80	0.870E-02	0.869E-02	0.373E-01
90	0.140E-01	0.140E-01	0.576E-01
100	0.210E-01	0.210E-01	0.842E-01
120	0.416E-01	0.416E-01	0.161E+00
140	0.728E-01	0.728E-01	0.276E+00
160	0.117E+00	0.117E+00	0.441E+00

(Table 3.2 is continued in the next page)

180	0.180E+00	0.177E+00	0.667E+00
200	0.324E+00	0.372E+00	0.970E+00

Table 3.3: Comparison of concentration values calculated by the Chebyshev pseudospectral method and the HOC scheme (for a period of *100yrs*)

Distance (m)	Exact	Chebyshev PS ($\Delta t = 0.001 \text{ yr}$)	HOCS ($\Delta t = 0.02 \text{ yr}$)
10.0	0.7143E+00	0.7143E+00 (0.5263E-04)	0.7143E+00 (0.3563E-02)
20.0	0.4653E+00	0.4653E+00 (0.1801E-03)	0.4653E+00 (0.6305E-02)
30.0	0.2709E+00	0.2709E+00 (0.4959E-03)	0.2709E+00 (0.5015E-02)
40.0	0.1391E+00	0.1391E+00 (0.1201E-02)	0.1391E+00 (0.4671E-02)

(Table 3.3 is continued to the next page)

50.0	0.6229E-01	0.6228E-01 (0.2616E-02)	0.6230E-01 (0.2934E-01)
60.0	0.2402E-01	0.2402E-01 (0.5215E-02)	0.2404E-01 (0.8175E-01)
70.0	0.7890E-02	0.7889E-02 (0.9670E-02)	0.7905E-02 (0.1892E+00)
80.0	0.2183E-02	0.2182E-02 (0.1689E-01)	0.2191E-02 (0.4072E+00)
90.0	0.5029E-03	0.5027E-03 (0.2809E-01)	0.5071E-03 (0.8396E+00)
100.0	0.9544E-04	0.9540E-04 (0.4482E-01)	0.9703E-04 (0.1664E+01)
110.0	0.1476E-04	0.1475E-04 (0.6904E-01)	0.1523E-04 (0.3164E+01)
120.0	0.1840E-05	0.1838E-05 (0.1032E+00)	0.1946E-05 (0.5769E+01)

(Table 3.3 is continued in the next page)

130.0	0.1829E-06	0.1826E-06 (0.1502E+00)	0.2014E-06 (0.1012E+02)
140.0	0.1434E-07	0.1431E-07 (0.2137E+00)	0.1680E-07 (0.1717E+02)
150.0	0.8774E-09	0.8748E-09 (0.2979E+00)	0.1127E-08 (0.2840E+02)

3.8 References

- [1] H.O. Kreiss and J. Olinger, *Tellus.*, 24 (1972) 199.
- [2] B. Fornberg, On high order approximations of hyperbolic differential equations by a Fourier method, Report No. 39, Dept. Comput. Science, Uppsala University, 1972.
- [3] D. Funaro and D. Gottlieb, *Math. Comput.*, 51 (1988) 599.
- [4] D. Funaro and D. Gottlieb, *Math. Comput.*, 57 (1991) 585.
- [5] J. P. Boyd, *Chebyshev and Fourier spectral methods*, Dover, New York, 2000.
- [6] J.P. Boyd, *J. Comput. Phys.* 103 (1992) 243.
- [7] J.P. Boyd, *Appl. Numer. Math.* 7 (1991) 287.
- [8] J.P. Boyd, *Comput. Methods Appl. Mech. Eng.* 116 (1994) 1.
- [9] W.S. Don and D. Gottlieb, *SIAM J. Numer. Anal.*, 31 (1994) 1519.
- [10] J. Shen, *Proceedings of ICOSAHOM '95*, *Houston J. Math.* (1996) 233.
- [11] H.P. Ma, *SIAM J. Numer. Anal.* 35 (1998) 869.
- [12] H.P. Ma, *SIAM J. Numer. Anal.* 35 (1998) 893.
- [13] H.P. Ma and W.W. Sun, *SIAM J. Numer. Anal.* 38 (2000) 1425.
- [14] D.W. Merrill, *Finite difference and pseudospectral methods applied to the shallow water equations in spherical coordinates*, Ph.D. Thesis, University of Colorado, 1997.
- [15] M. Ross and F. Fahroo, *Legendre pseudospectral approximations of optimal control problems*, *Lecture notes on control and information sciences*, Springer-Verlag, 295 (2003) 1.
- [16] M. Dehghan and M. Shamsi, *Numer. Meth. Partial D. E.* 22 (2006) 1255.
- [17] B.Y. Guoa and L.L. Wang, *J. Comput. Appl. Math.* 190 (2006) 304.

- [18] M. Javidi and A. Golbabai, *Appl. Math. Sci.* 1 (2007) 211.
- [19] M. Javidi and A. Golbabai, *J. Math. Anal. Appl.* 333 (2007) 1119.
- [20] A. Golbabai and M. Javidi, *Appl. Math. Comput.* 190 (2007) 179.
- [21] F.O. Akinpelu, L.A. Adetunde and E.O. Omidoira, *J. Appl. Sci. Environ. Mgt.* 9 (2005) 121.
- [22] C. Canuto, A. Quarteroni, M. Y. Hussaini and T. Zang, *Spectral Method in Fluid Mechanics*, Springer-Verlag, New York, 1988.

Chapter 4

Probabilistic estimation of the radioactivity migration

- 4.1 Introduction**
- 4.2 A brief survey of literature**
- 4.3 A description of our present model**
- 4.4 Results and discussions**
- 4.5 Conclusions**
- 4.6 References**

4.1 Introduction

This chapter deals with the probabilistic estimation of the radioactivity migration in a porous medium. In chapter 2, the deterministic parallel fracture model to estimate the migration of the radioactivity has been dealt with. There it is noted that a Laplace transform based analytical solution can be arrived at only when the source is assumed to be of constant strength. Moreover, this mode of solution has a major limitation with respect to the maximum distance of evaluation that turns out to be about $200m$ in quadruple precision. To extend the solution beyond this limit, four different finite difference approximations have been tried and the results are reported in chapter 2. These schemes do not suffer from this distance limitation to a larger extent and they can also handle a non constant source. But the finite difference schemes have limitations with respect to greater accuracy and the memory utilization. This was the motivation to use the two variants of a pseudospectral method which could provide accurate results up to $300m$. Although all these methods provide an estimation of the radioactivity migration, they still use a very simplified picture of a rock. The parallel fracture model is an idealization where the rock is thought to be a combination of an infinite array of identical parallel fractures separated by porous matrices of equal width.

In reality, a rock consists of porous blocks of uneven size in which several networks of randomly oriented and interconnected fractures are embedded. The schematic picture of a rock is given in fig. (1.1) of chapter 1. The pore water containing a radionuclide flows through these fractures. Due to the random network configuration, the effective path length traversed by the species from the source to an observation point located at the

z axis is higher than the linear distance between them. This will have an important bearing on the concentration. First, due to the increased path length, the concentration at a point of evaluation will be reduced. Secondly, with an increase in the path length, the retardation effects due to the porous matrix will also be enhanced. Hence due to these combined effects, the concentration will be significantly reduced and thus a realistic porous model will yield a less conservative estimate than the idealized parallel fracture model. *This is the motivation to address the present problem through a probabilistic route as the deterministic approach can not address this zigzag flow through a fracture network.*

An arbitrary single porous matrix with its embedded fracture network can be divided into several smaller blocks and the migration can be modeled by a random walk approach through this collection of smaller blocks. But as the number of porous matrices increases due to a larger domain as it happens in our case, the total number of smaller blocks increases enormously. Even though one can model the migration probabilistically in principle for this huge collection of blocks, in reality it becomes an impossible task. To circumvent this difficulty *we can assume that we can deal with a single porous matrix of an appropriate width* that reflects the averaging done over all the porous matrices of different shape, size and width that make up a real rock. We also calculate a quantity called the average migration length which is the average of several path lengths. With the average width and the average migration length, we can invoke the deterministic model to calculate required concentration profile as a function of time. Thus, we exploit the advantages of both the deterministic and the nondeterministic models.

4.2 A brief survey of literature

The probabilistic estimation of the migration of contaminant particles through a porous medium is a widely used technique. Using this approach, problems dealing with dispersion and diffusion have been handled since the middle of the last century ^[1, 2]. For our porous flow problem, a number of realistic models have been proposed based on the probabilistic estimation. Williams ^[3, 4] reported a stochastic approach to address the migration of radioactive waste through a fracture-porous matrix system. This was based on an analogy with the neutron transport in a non multiplying medium. He considers the transport of radionuclides in pore water as a series of linear movements through the randomly oriented and interconnected fractures. The radionuclide flow can encounter a sudden change of direction at a node which is the intersection point of two or more fractures. These are treated as pseudo-scattering events. He introduced a scattering term to quantify the reaction rate (like a particle getting deposited on a solid surface which amounts to a removal). The direction of the motion at a node is indicated by an anisotropy related function. Though this approach gives an analytic estimation of the transport through a fracture network, it has a serious drawback. The diffusion of species into the porous blocks from the fracture is not taken into consideration. The numerical solution of this model was reported in a series of papers by Buckley et al. ^[5, 6, 7].

The probabilistic model of Cvetkovic et al. ^[8] considered the migration in both the fractures and the porous matrices. He implemented the deterministic single fracture model in a small domain and considered the flow velocity as a truly random parameter and thus he repeats the calculation to cover the total volume of rock. For simplicity, he

ignored the diffusion process within a fracture and assumed that the transport was a function of advection alone. The results provided an estimation of the escape probability of a radioactive species from a rock.

In the model of Giacobbo and Patelli ^[9] the random walk of a particle in a phase space was governed by two quantities, a free flight kernel and a collision kernel characterizing a transition in the physical-chemical state of a particle (e.g. a particle encountering a node of fractures). They generated an effective path length between a source and an observation point using a random walk approach similar to that of Williams ^[3]. This model too did not consider the matrix diffusion but assumed a constant adsorption and desorption rate to account for the retardation offered by the porous matrices.

4.3 A description of our present model

Throughout the chapter, meter is used as the unit of length. As mentioned earlier, the radionuclide is assumed to travel through a network of interconnected fractures. This random network of fractures is embedded in porous matrices of random shapes and sizes. This is a very complicated system and the exact modeling of the migration involving the network of fractures and porous matrices is difficult. As explained in the third paragraph of this chapter, we introduce the average porous matrix width and the average migration length and then invoke the deterministic model. We assume a uniform distribution of the fractures and the porous blocks throughout the medium. That is, the average densities of the fractures and the porous blocks are independent of the position.

The migration of a radioactive particle through this network is modeled in two stages. In the first stage, a randomly oriented path between the source and the observation point is generated. Following Williams ^[3], we assume that the flow through a network can be imagined as a series of straight line movements. The radionuclide can change its direction only at a node which is the intersection of two or more fractures. Thus there is no change of direction of movement between two consecutive nodes. In a practical situation, the shape, the width and the length of a fracture vary randomly. For simplicity, we assume that the first two quantities are identical for all the fractures whereas the length is assumed to follow a distribution. Buckley et al. ^[6] considered two models namely, the Picket Fence and the Fracture Angle models to sample the fracture length. By analogy with neutron transport, a term called the mean free path was introduced in these models. This is the average distance that a particle travels between two consecutive pseudo-scattering events. Cvetkovic et al. ^[8] assumed a uniform distribution of fracture length in the interval $[l, l_0]$ and we follow the same distribution.

The next point to be considered is the orientation of a fracture at each node. The Fracture Angle model ^[6] assumes that at each node a fracture can have a orientation (with respect to the mean flow direction) that is uniformly distributed in the range $[-\varphi_{max}, \varphi_{max}]$. The same assumption was considered by Giacobbo and Patelli ^[9]. Now this angle that defines the new direction of flow at a node is called the *branching angle*. Using the above defined quantities, one can generate a *migration length* that a particle travels between the source and the observation point. By repeating this a number of times, we obtain an

average migration length. The steps involved in this statistical averaging are described below.

- a. Sample a set of fracture lengths from a uniform distribution in the range $[l, 10l]$.
- b. Sample a set of branching angles from the range $[-\varphi_{max}, \varphi_{max}]$.
- c. Select a fracture length and a corresponding branching angle from these two sets defined in the previous two steps.
- d. The selected fracture is of length L_f and it is oriented at an angle φ with respect to the mean flow direction. Then it has a projection of magnitude $L_f \cos(\varphi)$ in the mean flow direction. To cover a distance of length L_{SD} between the source and the observation point along the mean flow direction, one has to repeat steps (c) and (d) till the quantity $(\sum_i L_f^i \cos(\varphi^i))$ equals L_{SD} .
- e. Steps from (a) till (d) will generate a *value* for the migration length. This is repeated a number of times to arrive at the *average migration length* between the source and the observation point.

The second stage of the modeling involves the migration of the radioactive species through the porous matrix by choosing an average width and then use it along with average migration length in the deterministic model. We choose this truly random quantity as follows. Let $L_{f,max}$ denote the maximum length of a fracture and φ_{max} denote the maximum branching angle for a rock sample. Then the maximum possible distance of separation of two consecutive fractures is $\Delta = 2L_{f,max}\sin(\varphi_{max})$ (fig. 4.1). On the other hand, the minimum distance of separation is zero (at a node). This implies that the average width of the porous matrix must fall in between 0 and Δ . We choose uniformly

distributed values from the interval $[0, \Delta]$ to represent the average width of the porous matrix.

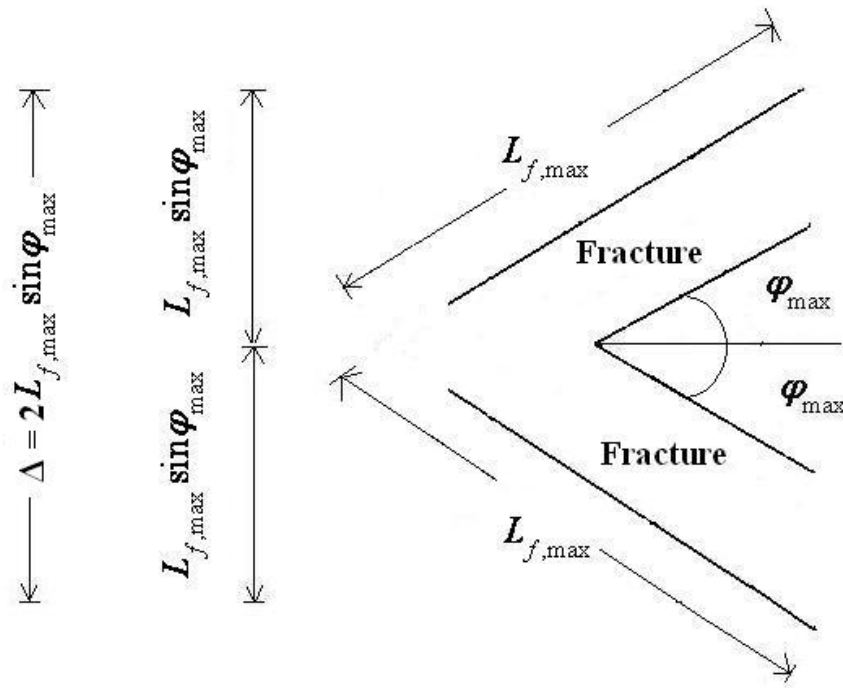


Fig. 4.1: Estimation of the maximum width of a porous matrix

With the average porous matrix width and the average migration length, we solve the coupled pde's that were solved in second chapter using the same set of parameters that were used earlier [eq. (2.9) and eq. (2.19)].

4.4 Results and discussions

All the calculations reported in this chapter are performed in double precision for a period of 1000 yr. Three sets of values are chosen for φ_{max} namely 30° , 60° and 89° . For each of these values, we have followed the steps from (a) to (e) described in the previous section to arrive at an average migration length. The *law of large numbers* ^[10] states that the average of a set of independent and identically distributed random numbers tends to a mean value with an increase in the size of the sample space. In this present problem if the number of trials exceeds about 10^4 , we arrive at a mean value for the average migration length. Hence for all the values of φ_{max} , 10^5 trials are performed to ensure a statistical convergence.

In the previous section, we have discussed in detail about the maximum and the minimum possible widths of the porous matrix for a rock sample. It was pointed out that the average width of a porous matrix is a function of φ_{max} and $L_{f,max}$. In this present study, we are using three different values of φ_{max} (30° , 60° and 89°) and $L_{f,max}$ is 10 in all the cases. So the maximum possible widths of the porous matrices are $10m$, $17.32m$ and $19.997m$ that correspond to $\varphi_{max} = 30^\circ$, 60° and 89° , respectively. Following the parallel fracture model, we denote the separation distance between the mid points of two consecutive fractures by $2B$. We choose $2B$ values from the set $\{1, 5, 10\}$ for all the values of φ_{max} . A radioactive element of very large half- life $T_{1/2} = 2.14E6$ is chosen so that the source strength can be considered as practically constant.

In figs.(4.2, 4.3) we plot the concentration as a function of the linear distance for all the values of φ_{max} . In these calculations, a fixed width of the porous matrix is considered. It is easy to note that there is a systematic decrease in the concentration value with the increase of φ_{max} . This can be understood very easily. A large φ_{max} will result in a large migration length and this in turn causes the reduction in the concentration values. For comparison, we have plotted the results of parallel fracture model for the same value of $2B$. In the figs.(4.2, 4.3), these values are labeled as 'Parallel frac'. As expected, the values of the standard parallel fracture model form an upper bound.

Next we study the effect of the width of the porous matrix on the concentration values. The results are plotted in figs.(4.4-4.6). It is important to note that in all the plots, the concentration values decrease with the increasing width of the porous matrix. Moreover, it reaches a saturation when the width exceeds the value 5. We can easily explain these trends. A porous matrix of large volume can allow more diffusion and absorption. This in turn causes the decrease in the concentration at the observation point. On the other hand, the diffusion process is limited up to a distance of few diffusion lengths. So beyond a limit, the concentrations saturate and this explains the patterns observed in figs.(4.4- 4.6).

4.5 Conclusions

The structure of a rock has a complicated randomness and the modeling of the migration of a species through this medium demands a huge computational effort. We have tried to model realistically this complex mechanism subject to the limits of practical

computation. In this process, the ingredients from both the probabilistic and the deterministic approaches are used. We have used two randomly varying parameters, namely the fracture length and the branching angle and both of them are assumed to follow uniform distributions in their respective ranges. We attempt to mimic the migration of radioactivity within a rock by sampling over these two parameters. Subsequently, the calculations are performed within the frame work of the deterministic parallel fracture model since this approach easily estimates the diffusion process through a porous block once the width of the porous matrix is known. Thus by blending the best of the deterministic and the probabilistic approaches, we try to improve the results of the simplified parallel fracture model.

From the results, it can be noted that the current approach gives a less conservative estimate when compared to its deterministic counterpart. This reduction of conservatism of concentration estimates is very desirable from both the radiological and environmental angles. The present model can be definitely improved if an analytical solution for a finite fracture embedded in a finite porous matrix is possible. As far we know, such solution is *not* available. This needs to be explored in future. If such a solution is made possible, then each segment of the zizzag path can be handled by this proposed new solution technique. This suggested approach will prove to be a much better probabilistic model of the porous medium than the present one that we have just indicated. Also, our present model has assumed a constant source. This is only to use the analytical results of the constant source parallel fracture model. Instead, if we resort to a finite difference solution for the parallel fracture model, then the requirement of a

constant source can be avoided. As a final remark, it must be mentioned that only experimental results can truly test the merits of all these models.

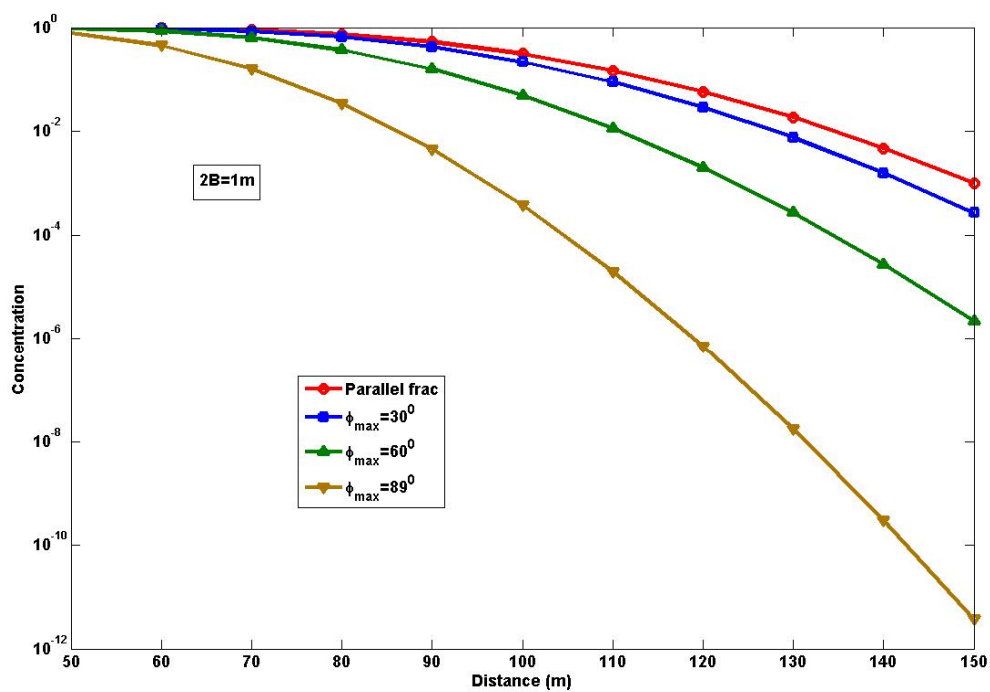
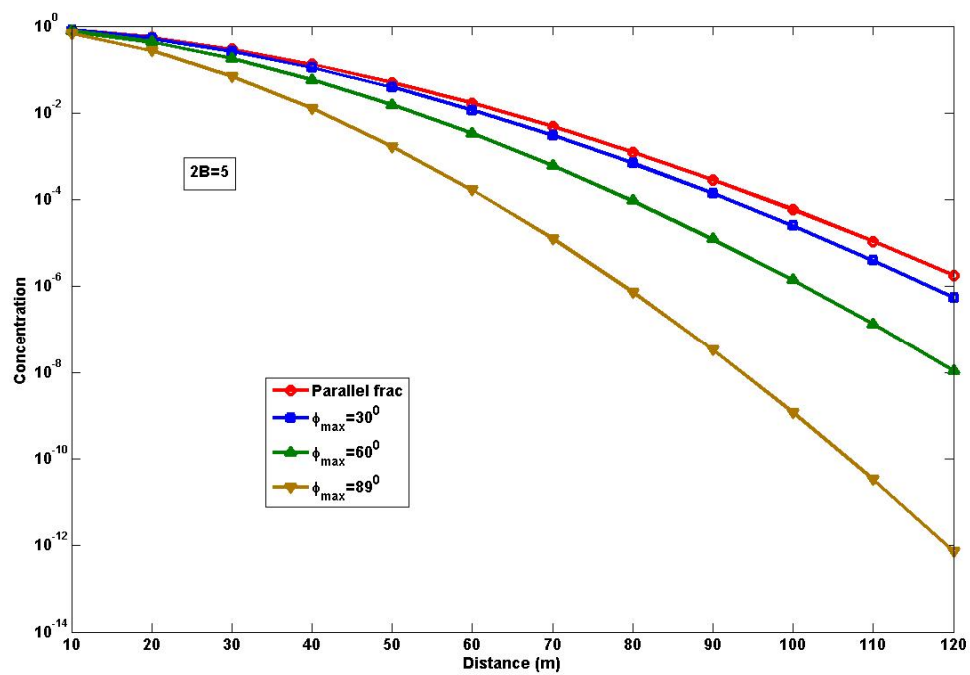
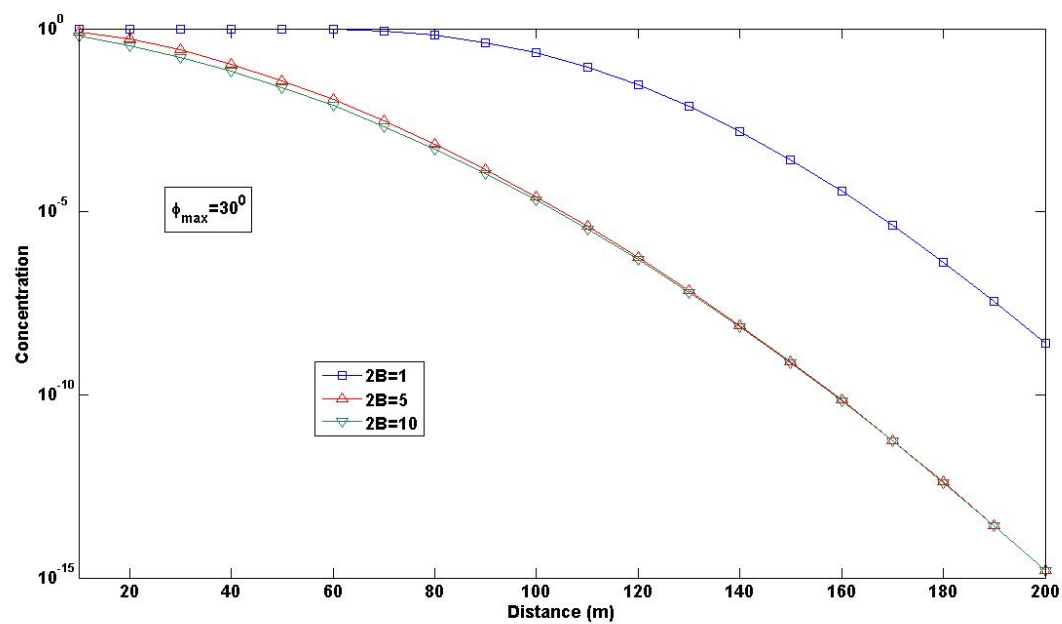


Fig. 4.2: Concentration vs. distance plot for $2B = 1$.

Fig. 4.3: Concentration vs. distance plot for $2B = 5$.Fig. 4.4: Concentration vs. distance plot for $\phi_{max}=30^\circ$

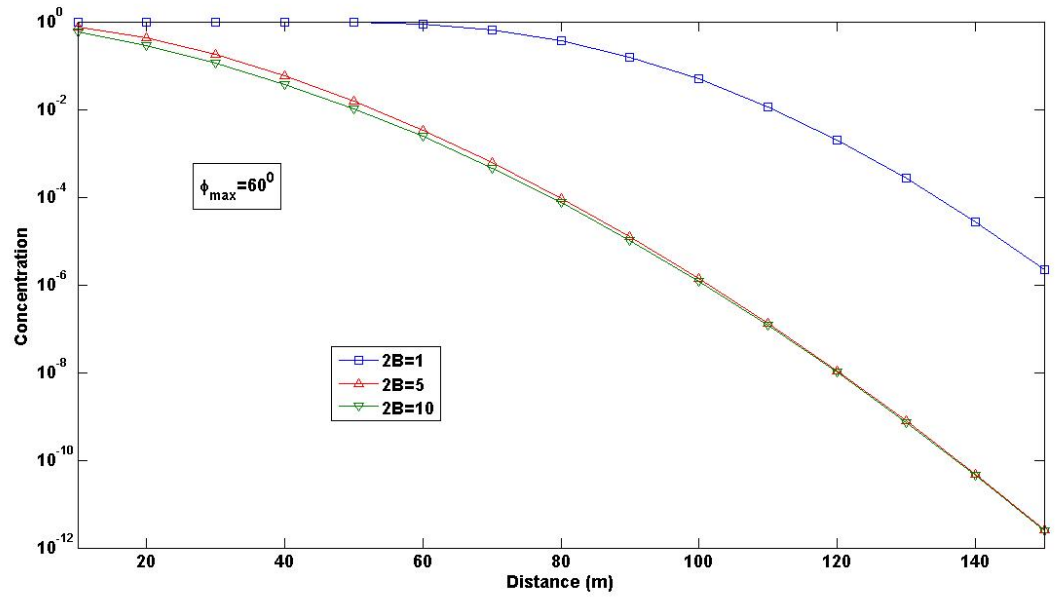


Fig. 4.5: Concentration vs. distance plot for $\phi_{max} = 60^\circ$

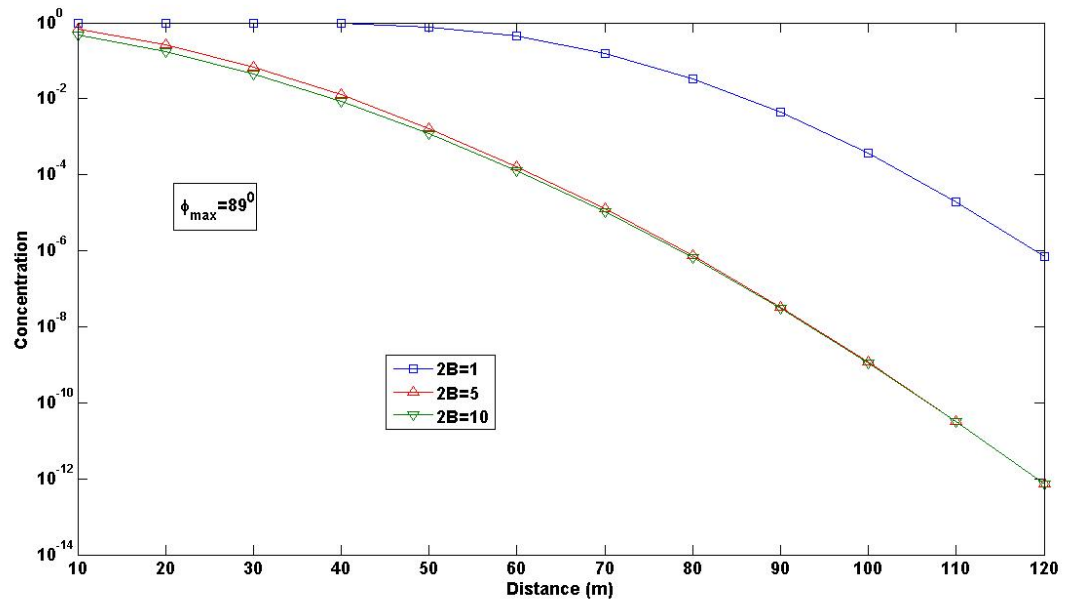


Fig. 4.6: Concentration vs. distance plot for $\phi_{max} = 89^\circ$

4.6 References

- [1] A.E. Scheidegger, *J. Geophys. Res.* 66 (1954) 3273.
- [2] G.D.J. de Jong, *Trans. Am. Geophys. Union* 39 (1958) 67.
- [3] M.M.R. Williams, *Ann. Nucl. Energy* 19 (1992) 791.
- [4] M.M.R. Williams, *Ann. Nucl. Energy* 20 (1993) 185.
- [5] R.L. Buckley, S.K. Loyalka and M.M.R. Williams, *Ann. Nucl. Energy* 20 (1993) 203.
- [6] R.L. Buckley, S.K. Loyalka and M.M.R. Williams, *Ann. Nucl. Energy* 20 (1993) 421.
- [7] R.L. Buckley, S.K. Loyalka and M.M.R. Williams, *Ann. Nucl. Energy* 20 (1993) 569.
- [8] V. Cvetkovic, S. Painter and J.O. Selroos, *Nucl. Sci. Eng.* 142 (2002) 292.
- [9] F. Giacobbo and E. Patelli, *Ann. Nucl. Energy* 35 (2008) 1732.
- [10] W. Feller, *An introduction to probability theory and its applications*, vol.I, third ed. Wiley-India, New Delhi. 2008.

Chapter 5

Numerical experimentation with the CN scheme

- 5.1 Introduction**
- 5.2 The CN and the ICN scheme**
- 5.3 The GCN scheme**
- 5.4 Test problems**
- 5.5 The migration of radioactivity in a porous medium**
- 5.6 Conclusions**
- 5.7 References**

5.1 Introduction

The Crank-Nicolson (CN) scheme is one of the widely used finite difference schemes ^[1]. It finds extensive application in the numerical solution of partial differential equations (pde's) dealing with the diffusion problems and similar ones relating to pricing options in finance. It is unconditionally stable and it is capable of second order accuracy in both the space and the time variables. However it has a particular limitation. The solution values are prone to oscillations at times ^[2]. This gave the starting point to look for improvements and alternatives that would eliminate or minimize these oscillations. This led to certain numerical experiments wherein a variant of the existing CN method was developed. This new variant retains the advantages of the classical CN method and yet promises few additional benefits. This new variant of the CN method is called the Generalized CN (GCN) scheme. Specifically, this new variant exhibits a more robust convergence pattern. That is, even though both the CN and the GCN methods eventually converge to the same value with nearly equal time steps, *the onset of solution is quite early for the new generalization*. The material is organized as follows. We briefly discuss the CN method and then indicate the new approach. This is followed by a stability analysis and finally, we present few test cases where we compare the new and the old schemes.

5.2 The CN and the ICN schemes

C_i^j denotes the unknown $C(i\Delta z, j\Delta t)$ where z and t refer to the space and the time variables, respectively. In the CN scheme, the time derivative of $C(z,t)$ is approximated simply as

$$\frac{\partial C_i^j}{\partial t} \approx \frac{C_i^{j+1} - C_i^j}{\Delta t} \quad (5.1)$$

The discretized quantities on the rhs of the above equation are centered around the half-integer time $(j + 1/2) \Delta t$. The first and second space derivatives are approximated by a central difference formula below and *by construction*, these discretized quantities too are centered around the same time $(j + 1/2) \Delta t$.

$$\frac{\partial C_i^j}{\partial z} \approx (1/2) \left\{ \frac{C_{i+1}^j - C_{i-1}^j}{2\Delta z} + \frac{C_{i+1}^{j+1} - C_{i-1}^{j+1}}{2\Delta z} \right\} \quad (5.2)$$

$$\frac{\partial^2 C_i^j}{\partial z^2} \approx (1/2) \left\{ \frac{C_{i+1}^j - 2C_i^j + C_{i-1}^j}{(\Delta z)^2} + \frac{C_{i+1}^{j+1} - 2C_i^{j+1} + C_{i-1}^{j+1}}{(\Delta z)^2} \right\} \quad (5.3)$$

The CN scheme allows an alternate approximation where all the derivative quantities are centered around the integer time $(j\Delta t)$ instead of $(j + 1/2)\Delta t$. We denote this integer time centered scheme as the ICN method for convenience and below we indicate this discretization.

$$\frac{\partial C_i^j}{\partial t} \approx \frac{C_i^{j+1} - C_i^{j-1}}{2\Delta t} \quad (5.4)$$

$$\frac{\partial C_i^j}{\partial z} \approx (1/2) \left\{ \frac{C_{i+1}^{j-1} - C_{i-1}^{j-1}}{2\Delta z} + \frac{C_{i+1}^{j+1} - C_{i-1}^{j+1}}{2\Delta z} \right\} \quad (5.5)$$

$$\frac{\partial^2 C_i^j}{\partial z^2} \approx (1/2) \left\{ \frac{C_{i+1}^{j-1} - 2C_i^{j-1} + C_{i-1}^{j-1}}{(\Delta z)^2} + \frac{C_{i+1}^{j+1} - 2C_i^{j+1} + C_{i-1}^{j+1}}{(\Delta z)^2} \right\} \quad (5.6)$$

5.3 The GCN scheme

The new GCN scheme that we introduce is just a simple arithmetic average of the CN and the ICN schemes *after* we have discretized the given pde. This we illustrate with the following simple one dimensional diffusion problem.

$$\frac{\partial C}{\partial t} - \frac{\partial^2 C}{\partial z^2} = 0 ; 0 \leq z \leq L ; t \geq 0 \quad (5.7)$$

Using the CN scheme, above equation gets discretized as

$$-K_1 C_{i-1}^{j+1} + (1 + 2K_1) C_i^{j+1} - K_1 C_{i+1}^{j+1} = K_1 [C_{i-1}^j - 2C_i^j + C_{i+1}^j] + C_i^j ; K_1 = \frac{\Delta t}{2(\Delta z)^2} \quad (5.8)$$

Similarly, using the ICN scheme, we get the following equation.

$$-K_2 C_{i-1}^{j+1} + (1 + 2K_2) C_i^{j+1} - K_2 C_{i+1}^{j+1} = K_2 [C_{i-1}^{j-1} - 2C_i^{j-1} + C_{i+1}^{j-1}] + C_i^{j-1} ; K_2 = \frac{\Delta t}{(\Delta z)^2} \quad (5.9)$$

Now in the GCN scheme, we average both the discretized equations indicated above to get the following expression.

$$\begin{aligned} & -(K_1 + K_2) C_{i-1}^{j+1} + (2 + 2K_1 + 2K_2) C_i^{j+1} - (K_1 + K_2) C_{i+1}^{j+1} \\ & = K_1 [C_{i-1}^j - 2C_i^j + C_{i+1}^j] + C_i^j + K_2 [C_{i-1}^{j-1} - 2C_i^{j-1} + C_{i+1}^{j-1}] + C_i^{j-1} \end{aligned} \quad (5.10)$$

For the pde given by eq. (5.7), let us consider the standard Von Neumann stability analysis^[1]. We set

$$C_n^j = (\rho)^j \exp(ikn\Delta z)$$

where k is the wave number and ρ is the error amplification factor. Upon substituting the above expression in the three finite difference schemes under consideration, we arrive at the following expressions for the amplification factor.

$$\rho_{CN} = \frac{1 - 4\alpha\beta}{1 + 4\alpha\beta} \quad (5.11)$$

$$\rho_{ICN} = \sqrt{\frac{1 - 8\alpha\beta}{1 + 8\alpha\beta}} \quad (5.12)$$

$$\rho_{GCN} = \frac{(1 - 4\alpha\beta) \pm \sqrt{(1 - 4\alpha\beta)^2 + 4(1 - 8\alpha\beta)(2 + 12\alpha\beta)}}{2(2 + 12\alpha\beta)} \quad (5.13)$$

where,
$$\alpha = \frac{\Delta t}{2(\Delta z)^2} ; \beta = \sin^2(k\Delta z / 2) \quad (5.14)$$

Numerical stability of the discretization demands that the modulus of the amplification factor is bounded by unity so that the errors do not multiply as the computation progresses. Note that for a fixed Δz , α varies linearly as Δt . Now as the time step $\Delta t \rightarrow 0$, then $\alpha \rightarrow 0$, it is found that both ρ_{CN} and ρ_{ICN} tend to unity. ρ_{GCN} tends to 1 or (-0.5). On the other hand for large time steps, that is when α tends to infinity, both ρ_{CN} and ρ_{ICN} tend to unity. However, in this case, $|\rho_{GCN}|^2 \rightarrow \frac{2}{3}$. Hence *all the three schemes are unconditionally stable for the given problem*. Moreover, since the magnitude of the amplification factor of the new scheme is less than unity, *the GCN method promises the possibility of an early onset of solution* which makes the convergence more robust in comparison with the other two variants. Now let us list out the truncation errors (T.E.) of all the three variants of CN schemes.

$$(T.E.)_{CN} = \frac{(\Delta t)^2}{6} \frac{\partial^3 C}{\partial t^3} - \frac{(\Delta t)^2}{4} \frac{\partial^4 C}{\partial z^2 \partial t^2} - \frac{(\Delta z)^2}{12} \frac{\partial^4 C}{\partial z^4} + O\left[(\Delta z)^3, (\Delta t)^3\right] \quad (5.15)$$

$$(T.E.)_{ICN} = \frac{(\Delta t)^2}{6} \frac{\partial^3 C}{\partial t^3} - \frac{(\Delta t)^2}{2} \frac{\partial^4 C}{\partial z^2 \partial t^2} - \frac{(\Delta z)^2}{12} \frac{\partial^4 C}{\partial z^4} + O\left[(\Delta z)^3, (\Delta t)^3\right] \quad (5.16)$$

$$(T.E.)_{GCN} = \frac{(\Delta t)^2}{6} \frac{\partial^3 C}{\partial t^3} - \frac{3(\Delta t)^2}{8} \frac{\partial^4 C}{\partial z^2 \partial t^2} - \frac{(\Delta z)^2}{12} \frac{\partial^4 C}{\partial z^4} + O\left[(\Delta z)^3, (\Delta t)^3\right] \quad (5.17)$$

The three schemes are compared first for two simple diffusion problems over finite domains with different initial and boundary conditions. These two problems ^[3] are indicated below.

5.4 Test Problems

Test problem 1.

$$\frac{\partial C}{\partial t} - \frac{\partial^2 C}{\partial x^2} = 0 ; 0 < x < \pi ; t > 0 \quad (5.18)$$

The boundary conditions are

$$C(0, t) = 0 ; t > 0 \quad (5.19)$$

$$C(\pi, t) = 0 ; t > 0 \quad (5.20)$$

The initial condition is given by

$$C(x, 0) = x(\pi - x) ; \pi \geq x \geq 0 \quad (5.21)$$

The exact solution is given by

$$C(x, t) = \frac{8}{\pi} \sum_{n=1}^{\infty} \frac{\sin[(2n-1)x]}{(2n-1)^3} \exp[-(2n-1)^2 t] \quad (5.22)$$

Test Problem 2.

$$\frac{\partial C}{\partial t} - \frac{\partial^2 C}{\partial x^2} = 0 ; 0 < x < L ; t > 0 \quad (5.23)$$

The initial condition is given by

$$C(x, 0) = x ; L \geq x \geq 0 \quad (5.24)$$

The boundary conditions are given by

$$\frac{\partial C(0, t)}{\partial x} = 0 ; t > 0 \quad (5.25)$$

$$C(L, t) = 0 ; t > 0 \quad (5.26)$$

The exact solution is given by

$$C(x,t) = -\frac{4L}{\pi} \sum_{n=1}^{\infty} \left[\frac{2}{(2n-1)^2 \pi} + \frac{(-1)^n}{2n-1} \right] \cos \left[\frac{(2n-1)\pi x}{2L} \right] \exp \left[\frac{-(2n-1)^2 \pi^2 t}{4L^2} \right] \quad (5.27)$$

The comparison of the results for these problems is indicated in table 5.1 and table 5.2. For the first problem, when the time step has the value $\Delta t = 0.2$, the values of the GCN schemes are definitely *closer* to the exact values than those of the CN schemes as seen from table 5.1. Also, the ICN scheme fails to converge with this time step value. Subsequently, with $\Delta t = 0.05$, all the three schemes converge to nearly the same value. Thus the relatively more robust convergence of the GCN scheme is obvious. A similar trend is manifested in the results of the test problem 2. The values from the GCN scheme start appearing with the time steps $\Delta t = 0.05$, $\Delta t = 0.01$ when the other two methods have not converged at this stage. The non-availability of the results for these time steps for the CN and ICN schemes are indicated by the symbols * and ** in the third and fourth columns, respectively. All the three schemes converge eventually to roughly the same value with $\Delta t = 0.002$. The ICN scheme does not exhibit a convergence with $\Delta t = 0.005$. The GCN values with $\Delta t = 0.01$ are not different from the values of CN schemes with $\Delta t = 0.005$. The relatively robust convergence of the GCN scheme is apparent. Lastly, it must be remarked that for the second test problem, the exact values given in the second column of table 5.2 differs from the converged values of all the three schemes under consideration.

5.5 The migration of radioactivity in a porous medium

Next we consider the solution of the pde's of the parallel fracture model for the migration of radionuclides that has been dealt with in the second and third chapters. The governing pde's are given below. The initial, boundary and inlet conditions are the same as in our earlier chapters.

$$\frac{\partial C}{\partial t} + \frac{v}{R} \frac{\partial C}{\partial z} - \frac{D}{R} \frac{\partial^2 C}{\partial z^2} + \lambda C + \frac{q}{Rb} = 0, \quad z \geq 0, \quad t \geq 0 \quad (5.28)$$

$$\frac{\partial C_p}{\partial t} - \frac{D_p}{R_p} \frac{\partial^2 C_p}{\partial x^2} + \lambda C_p = 0, \quad b \leq x \leq B, \quad t \geq 0 \quad (5.29)$$

The solution is needed for fairly large distances like $z = 500m$ and for longer times that are governed by the half-lives of the radioactive species. Hence the number of grid points is fairly large. Hence this practically important problem calls for accurate solutions with computational economy. The superiority of the GCN scheme over the other two schemes is brought out well in this problem. In table 5.3, the computations are done with three different time steps, namely, $\Delta t = 0.2, 0.05, 0.02$ yr. It can be noted that the values calculated by the ICN scheme are not stable for this problem and so they are not included in table 5.3. When the time step is $\Delta t = 0.2$ yr, the GCN and the CN results converge but for large distances ($z \geq 300m$), the results of the CN method deviate by *one or five orders*. On the contrary, the order estimates of the GCN values for this fairly large time step is not in error demonstrating once again the early convergence. Again, GCN values corresponding to time steps $\Delta t = 0.05$ yr and 0.02 yr do not differ much.

Finally, these schemes were compared for the following simple problem when both the advection and the diffusion were involved ^[4]. The results for this case are similar to those of the test problems 1 and 2.

$$\frac{\partial C}{\partial t} + \beta \frac{\partial C}{\partial x} - \alpha \frac{\partial^2 C}{\partial x^2} = 0 ; 0 \leq x \leq L ; t \geq 0 \quad (5.30)$$

The initial condition is given below.

$$\varphi(x) = \exp \left[-\frac{(x-\beta)^2}{4\alpha} \right] \quad (5.31)$$

The boundary conditions are given below.

$$C(0,t) = \frac{1}{\sqrt{1+t}} \exp \left[-\frac{(1+t)^2 \beta^2}{4(1+t)\alpha} \right] ; t \geq 0 \quad (5.32)$$

$$C(L,t) = \frac{1}{\sqrt{1+t}} \exp \left[-\frac{\{L-(1+t)\beta\}^2}{4(1+t)\alpha} \right] ; t \geq 0 \quad (5.33)$$

The exact solution is given below.

$$C(x,t) = \frac{1}{\sqrt{1+t}} \exp \left[-\frac{\{x-(1+t)\beta\}^2}{4(1+t)\alpha} \right] ; t \geq 0 \quad (5.34)$$

5.6 Conclusions

The new scheme GCN is a *better* variant of the conventional CN scheme. The convergence pattern of this scheme is definitely more robust than that of the CN and the ICN schemes. The amplification factor for the GCN scheme is smaller and this aids the onset of the solution for larger time steps while the conventional methods have not started

converging. Still one must admit that one does not gain a time step advantage since all the methods demand nearly the *same* time step for the *ultimate* convergence. The leading truncation error of the GCN scheme is just the arithmetical average of the CN and the ICN schemes and hence this error quantity is roughly the same in all the three cases and this has a bearing on the time step requirement for the ultimate convergence. This being said, *for complicated phenomena the estimates of the new scheme can be more relied upon since the convergence is definitely more robust in this case as demonstrated in the porous flow case.* Still, a lot more experimentation and more elaborate error analysis are needed to exploit the full potential of this new scheme. These aspects will be pursued in a future work.

Table 5.1: The concentration values at different distances by conventional CN, GCN and ICN methods, $NX = 11$, time = 20. (test problem 1)

X	Exact (E-08)	GCN (E-08) $\Delta t = 0.2$	CN (E-08) $\Delta t = 0.2$	ICN (E-08) $\Delta t = 0.2$	GCN (E-08) $\Delta t = 0.05$	CN (E-08) $\Delta t = 0.05$	ICN (E-08) $\Delta t = 0.05$
0.31	0.162	0.154	0.179	0.189	0.190	0.188
0.63	0.309	0.293	0.340	0.359	0.362	0.358
0.94	0.425	0.403	0.469	0.494	0.498	0.492
1.26	0.499	0.473	0.551	0.580	0.586	0.579
1.57	0.525	0.498	0.579	0.610	0.616	0.608
1.88	0.499	0.473	0.551	0.580	0.586	0.579
2.20	0.425	0.403	0.469	0.494	0.498	0.492
2.51	0.309	0.293	0.340	0.359	0.362	0.358
2.83	0.162	0.154	0.179	0.189	0.190	0.188

Table 5.2: Concentration values at different distances by conventional CN, GCN and ICN methods, $L=1$, time=100, $NX=101$. (test problem 2)

X	Exact	GCN*	GCN**	GCN	CN	ICN	GCN	CN	ICN
	E-107	E-108	E-108	E-108	E-108	E-108	E-108	E-108	E-108
		$\Delta t =$ 0.05	$\Delta t =$ 0.01	$\Delta t =$ 0.005	$\Delta t =$ 0.005	$\Delta t =$ 0.005	$\Delta t =$ 0.002	$\Delta t =$ 0.002	$\Delta t =$ 0.002
0.1	0.318	0.100	0.259	0.266	0.268	0.268	0.268	0.266
0.2	0.306	0.097	0.249	0.257	0.258	0.258	0.259	0.256
0.3	0.287	0.091	0.234	0.240	0.242	0.242	0.242	0.240
0.4	0.260	0.082	0.212	0.219	0.220	0.220	0.220	0.218
0.5	0.227	0.072	0.186	0.191	0.192	0.193	0.193	0.191
0.6	0.189	0.060	0.154	0.159	0.160	0.160	0.160	0.159
0.7	0.146	0.046	0.119	0.123	0.123	0.124	0.124	0.123
0.8	0.099	0.032	0.081	0.084	0.084	0.084	0.084	0.083
0.9	0.050	0.016	0.041	0.042	0.043	0.043	0.043	0.042

The concentration values cannot be evaluated by CN and ICN with the time steps of GCN* and GCN**.

Table 5.3: Concentration values at different distances by conventional CN and GCN,
time= 1000yrs (NZ=2800, NX=5600) (The porous flow problem)

Z (m)	Exact	GCN	CN	GCN	CN	GCN	CN	GCN	CN
		$\Delta t = 0.2\text{yr}$	$\Delta t = 0.2\text{yr}$	$\Delta t = 0.05\text{yr}$	$\Delta t = 0.05\text{yr}$	$\Delta t = 0.02\text{yr}$	$\Delta t = 0.05\text{yr}$	$\Delta t = 0.02\text{yr}$	$\Delta t = 0.02\text{yr}$
20	3.63E-01	3.63E-01	3.63E-01	3.63E-01	3.63E-01	3.63E-01	3.63E-01	3.63E-01	3.63E-01
40	8.22E-02	8.22E-02	8.24E-02	8.22E-02	8.22E-02	8.22E-02	8.23E-02	8.22E-02	8.22E-02
60	1.12E-02	1.12E-02	1.13E-02	1.12E-02	1.12E-02	1.12E-02	1.12E-02	1.12E-02	1.12E-02
80	9.29E-04	9.35E-04	9.59E-04	9.35E-04	9.35E-04	9.35E-04	9.34E-04	9.35E-04	9.35E-04
100	4.79E-05	4.87E-05	5.13E-05	4.86E-05	4.86E-05	4.86E-05	4.85E-05	4.86E-05	4.86E-05
200	2.55E-14	3.04E-14	5.23E-14	2.95E-14	2.96E-14	2.93E-14	2.96E-14	2.95E-14	2.95E-14
300	1.69E-27	1.32E-26	1.50E-27	1.53E-27	1.47E-27	1.53E-27	1.47E-27	1.49E-27
400	3.10E-44	5.27E-42	2.31E-44	2.47E-44	2.17E-44	2.47E-44	2.17E-44	2.26E-44
500	6.67E-64	1.64E-59	3.64E-64	4.25E-64	3.22E-64	4.25E-64	3.22E-64	3.49E-64

5.7 **References**

- [1] E. Isaacson and H.B. Keller, Analysis of Numerical Methods, Dover, New York, 1994
- [2] D. J. Duffy, Wilmott Magazine 12 (2004) 68.
- [3] D. G. Duffy, Advanced Engineering Mathematics, CRC Press, USA, 1998.
- [4] A. Mohebbi, M. Dehghan, Appl. Math. Modell. 34 (2010) 3071.

Chapter 6

Conclusion and outline of the future work

6.1 Chapter wise summary of the thesis

6.2 Outline of future work

In this final chapter, we summarize the contents of all the previous chapters and then outline the problems that will be pursued as a sequel to the thesis investigations.

6.1 Chapter wise summary of the thesis

The first chapter gave a broader outline of the need for the present investigations. The ever increasing demand for energy in India will have a huge nuclear component in times to come. The reprocessing of the spent fuel from the reactors results in the high level wastes (HLW). The safe disposal of the HLW in a vitrified form in canisters in the underground repositories needs the present computational modeling of the radioactivity migration in a rock. An exhaustive survey of the existing literature dealing with both the deterministic and the nondeterministic models was presented.

In the second chapter, the basic physical model, the complete set of assumptions and a comprehensive derivation of the coupled pde's of the parallel fracture model were indicated. If the waste matrix has a constant strength, these pde's are solvable exactly by a Laplace transform technique. However, the evaluation of this elegant solution is beset with excessive numerical difficulties. To overcome this complication and to relax the requirement of a constant source, some of the state of the art finite difference schemes were tested. A higher order Crank-Nicolson scheme and a higher order compact finite difference scheme were shown to yield reliable concentration estimates for distances of the order of $500m$ or more. This must be contrasted with the analytical solution that can be obtained at best for a distance not exceeding $200m$.

In the third chapter, the numerical solution of the parallel fracture model is continued. The accuracy of the finite difference solutions still leaves a scope for improvement. Also, the memory utilization and the run time requirements are on the higher side for these schemes. So, the use of the pseudospectral methods is tested in this chapter. In particular, the Chebyshev and the Legendre pseudospectral methods are used and the accuracies offered by these methods surpass that of the finite difference schemes by one or two orders. This is due to the fact that the use of an appropriate basis functions guarantees an exponential convergence that is not possible for the finite difference schemes. Along with a superior accuracy, the runtimes and the memory requirements are drastically reduced. The runtime gets reduced by a factor of 72 and the memory requirement is curtailed by a big factor of 772. Due to an inherent limitation, this method can evaluate the concentration in quadruple precision up to a distance of about $300m$ only. Hence, for distances of this order, the pseudospectral method can be profitably used. For distances exceeding $300m$, the higher order Crank-Nicolson and the higher order compact finite difference methods can be chosen. Hence reliable prescriptions for the assessment of the concentration for distances like $500m$ are given within the framework of a standard deterministic model.

In the fourth chapter, the limitations of the deterministic model are improved by resorting to a nondeterministic model. Essentially, the deterministic model of a rock suffers from its simplicity. One needs to take into consideration a realistic structure of the rock with its porous matrices of random size in which random network of interconnected fractures are embedded. The straight line path connecting the source and the observation

point must be replaced by an average over several zigzag paths. Also, the radionuclide can go through any one of the branching paths (that is characterized by the term branching angle) at the intersection point of the fractures, called a node. In the nondeterministic model that is considered, a random walk approach is used. The linear distance between the source and the observation point is covered by a zigzag path and a segment of this path is called a fracture length. The sum of all these fracture lengths gives a quantity called the migration length. By repeating this process, different paths and hence a set of varying migration lengths are obtained. And finally after averaging, one gets an average migration length. By choosing an average porous matrix size, the parallel fracture model is employed to calculate the concentration where the distance is replaced by the average migration length. This approach, that effectively utilizes both the deterministic and the nondeterministic components tries to take into consideration the complex structure of the porous medium as realistically as possible, subject to the limitations of computation. One fruitful fallout of this method is the reduction of the conservatism in the assessment of the concentrations by the parallel fracture model. Since the path length is more in the nondeterministic route, there is a significant decrease in the concentration at the observation point. The increased path length also enhances the matrix retardation.

The fifth chapter is about numerical experiments involving the Crank-Nicolson (CN) schemes. Experimentation is driven by curiosity. The reason for the success of the classical CN scheme is due to the preservation of the same time centering in both the time and space derivative approximations. The CN scheme can be written down in two ways,

an integer time centered CN scheme and a half-integer time centered CN scheme. Given a pde, we can discretize it by both these schemes. In this process it occurred that by making an arithmetic average of these two discretizations for the same equation, one still maintains a time centering in both the time and space derivative approximations. Since this averaging involves more terms than the ones we started with, it may possibly yield better results. In fact numerical experiments indicate that this new CN variant is a better one than its original counterparts in an interesting way. The onset of correct solution values occurs for a larger time step while the other two methods still have not converged. However, for the eventual convergence, this new method needs the same time step and hence one does not get a time step advantage. More analysis and experiments are needed to exploit the full potential of this new variant. Interestingly, for pde's of our porous flow, this new method yields relatively better results.

6.2 Outline of future work

In the following, we indicate problems that can be pursued in future as a sequel to the present investigations.

- The parallel fracture model assumes a constant source and an exact solution is obtained via a Laplace transform method. This leads to an open problem where the constant source is replaced by a time varying source. A Fourier series type solution may be tried.
- Another interesting open problem is a single porous matrix of finite size with a fracture embedded in it. An analytical solution involving a Fourier series can be tried. Otherwise an efficient numerical solution can be worked out.

- If a practical solution can be obtained for the problem defined just above, then the infinite single porous matrix of a fixed width that is used in our random walk approach can be replaced by several porous matrices of *finite size and varying width*. This approach will be much more realistic since the present random walk model does not take into consideration finite porous matrices of varying sizes.
- The pseudospectral schemes employed in the thesis have excellent accuracy and need much reduced memory and run time. But they have a limitation with respect to the maximum distance of evaluation that is of the order of about *300m*. This condition needs to be relaxed if possible.
- The compact finite difference scheme employed in the thesis gives *4th* order accuracy in the space domain. This can be definitely extended to still higher orders.
- The use of Lattice Boltzmann methods for the migration involving a porous medium offers a novel possibility.
- The Crank-Nicolson variant needs further probing to exploit its full potential, especially if the time step related gains can be achieved.
- The stability analysis for the pseudospectral method is a quite demanding problem that needs to be investigated.
- Finally, setting up of some experimental facilities to validate these models is a very useful problem.

As a final remark, it must be pointed out that only the last mentioned future work relates to experiment. But such an experimental set up will really pave way for validating and improving the existing models in a practical and realistic way.